

See discussions, stats, and author profiles for this publication at: <https://www.researchgate.net/publication/318682766>

Nanotechnology and Nanomaterials for Improving Neural Interfaces

Article in *Advanced Functional Materials* · March 2018

DOI: 10.1002/adfm.201700905

CITATIONS

49

READS

901

6 authors, including:



Mian Wang

Northeastern University

35 PUBLICATIONS 928 CITATIONS

[SEE PROFILE](#)



Gujie Mi

Northeastern University

30 PUBLICATIONS 475 CITATIONS

[SEE PROFILE](#)



Di Shi

Northeastern University

34 PUBLICATIONS 512 CITATIONS

[SEE PROFILE](#)



Daniel James Hickey

Northeastern University

15 PUBLICATIONS 547 CITATIONS

[SEE PROFILE](#)

Some of the authors of this publication are also working on these related projects:



Nanoengineering of an Electroconductive Cardiac Patch [View project](#)



Aloe vera-mediated synthesis of metallic nanoparticles [View project](#)

Nanotechnology and Nanomaterials for Improving Neural Interfaces

Mian Wang, Gujie Mi, Di Shi, Nicole Bassous, Daniel Hickey, and Thomas J. Webster*

A successful biomaterial–neural tissue interface should demonstrate biocompatibility, cytocompatibility, the ability to integrate properly within neural tissues, and the prolonged maintenance of desired electrical properties. Neural electrodes implanted *in vivo* often experience degradation of these properties due to implant micromotion, mechanical mismatch, an extensive foreign-body response, and the formation of glial scar tissue that interfere with signal transmission. However, recent advances in nanotechnology and nanomaterials show great promise to address these problems due to their biologically inspired surface features and enhanced electrical properties. This review will discuss how nanomaterials and nanotechnology are being used to fabricate advanced neural electrodes that demonstrate greater bio-integration properties, enhanced prolonged electrical properties, and an improved signal specificity down to the single molecule range. First, an overview of current biomaterial–neural tissue interface technology is provided, followed by an examination of conventional and newly developed micro- and nano-fabrication methodologies. Nanomaterials that have shown the most promise for neural interfacial applications are then discussed, including carbon nanomaterials, conductive polymers, and hybrid nanomaterials. The purpose of this review is to describe recent advances in nanotechnology for improved biomaterial–neural tissue interfaces, and identify their advantages and disadvantages from a researcher's perspective.

1. Introduction

The human brain is characteristically actuated by billions of neurons that interact to regulate mechanical or sensory behaviors. These behaviors are confined to wired activity of the senses, muscular response catalysis, memory formation, and, more generally, guided behavior. Extensive research has been conducted to achieve a deeper understanding of inter-neural interactions. For example, in 1875, using galvanometric

analysis, Richard Caton first described how current variations in the brain correlate to observable behaviors. Hans Berger then developed the first electrocorticogram for monitoring the electrical activity of the electrode-appended brain.^[1,2] His examination of electroencephalogram data enabled him to define the sensitivity constraints prescribed by α and β brain wave patterns.^[2] Subsequent efforts contributed to the development of the neuroscience field as we recognize it today.

Perhaps the most important advance in the study and treatment of the brain is the development of the neural interface. Neural interfaces establish direct communication between the central nervous system (CNS) and a sovereign, man-made digital system.^[3] Such interfaces promote a neurophysiological understanding and provide a clinical means for detecting or treating neurological symptoms and diseases. Neural interfaces, or brain-machine interfaces (BMIs), can preserve the function of impaired neuronal tissues by translating nervous system signals into quantities that can be computationally understood.^[4] The comprehensive


BMI design principle is to augment or restore one or more of the three interrelated biological complications that arise from neural impairment: sensory malfunction, loss of motor control, or disease-elicited intellectual changes.^[3] The success of such a device relies on understanding the principles of bioelectrical transduction, neural modulation through computational calibration, and acclimating signal processing.

Three different classes of BMIs—sensory, motor, and cognitive—were designed with exclusive parameters for sustaining competent cerebral operation.^[3] Sensory BMIs demonstrate the ability to deliver stimuli to domestic cortices for the correction of occipital, somatosensory, and/or auditory complications. Currently, the most common sensory neural interfaces are cochlear implants, which correct processing complications of the tonotopic space.^[3] These devices are assembled using small-scale microphones and signal processors that translate sound waves into neuronal responses, and thus enable hearing. Alternatively, retinal prostheses are being developed to translate external morphological content into sensory firings that could be perceived by patients suffering from blindness.^[5]

Moreover, deficits associated with the limbic system could potentially be repaired using cognitive BMIs. Cognitive BMIs

M. Wang, G. Mi, D. Shi, N. Bassous, D. Hickey, Prof. T. J. Webster
Department of Chemical Engineering
Northeastern University
Boston, Massachusetts, USA
E-mail: th.webster@neu.edu

Prof. T. J. Webster
Wenzhou Institute of Biomaterials and Engineering
Wenzhou Medical University
Wenzhou, Zhejiang, China

 The ORCID identification number(s) for the author(s) of this article can be found under <https://doi.org/10.1002/adfm.201700905>.

DOI: 10.1002/adfm.201700905

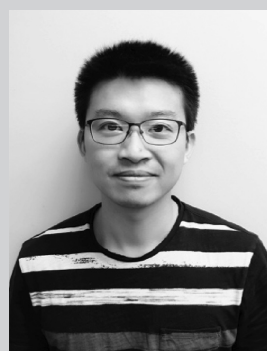
for treating Alzheimer's disease, for example, are designed to restore communication among damaged or disparate neural networks.^[6] Motor BMIs, on the other hand, are engineered to reestablish communication between the CNS and the organs or muscles of the peripheral nervous system that have lost functional mobility. Such devices could be critical for patients suffering from neurodegenerative disorders like cerebral palsy, amyotrophic lateral sclerosis, stroke, or traumatic injury.^[7] External motor BMIs ideally retrieve action-control commands from the brain to electrically stimulate prosthetic implants or native biological tissue.^[8] Ultimately, multidisciplinary efforts in neurophysiology and engineering are necessary to establish systems that can mimic the sensory pathways of the brain and process external or internal stimuli. This review will focus on materials recently developed, specifically at the nanoscale, that vastly enhance electrical properties, mechanical properties, location specificity, cytocompatibility and biocompatibility to advance our understanding of the CNS and enable greater control over diseased/damaged states compared to current technologies.

2. Current Status of the Biomaterial Neural Tissue Interface

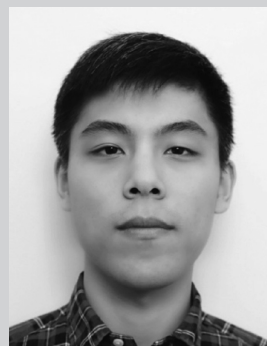
2.1. Conventional Biomaterial Neural Tissue Interface Technologies

The development of biomaterial neural tissue interfaces has been largely influenced by the use of electrophysiology to extract electroencephalogram (EEG)^[9] and electrocorticogram (ECoG)^[10] recordings, in addition to action potential spikes^[11] and local field potential data.^[12] A comparison of the placement and signal resolution between three classes of neural interfaces is presented in **Figure 1**. The most basic, noninvasive methodology for collecting neuronal signals is the EEG, which has been applied for diagnosing epilepsy, enhancing our understanding of language perception, monitoring sleep, and measuring cognitive indicator remittance.^[13–16] Despite the many advances in neurology made possible by EEG and other non-invasive recording methods, there are several limitations to these technologies. For instance, traditional EEG devices suffer from low transfer rates, on the order of 5–25 bit s⁻¹.^[11,17,18] Additionally, because EEG electrodes are simply affixed to the scalp, the densely packed tissues of the brain, cranium, and skin act as barriers that impede signal transduction to the external electrode, thus limiting the spatial and temporal resolution of the EEG results. Artifacts due to electrical stimulation, electromyographic activity, and mechanical disturbances further interfere with EEG resolution.^[11] Due to the poor resolution of EEG-based systems, recent trends have examined the use of more invasive neural interface technologies like the ECoG.

Relative to the EEG, ECoG is capable of recording higher frequency data with greater accuracy and with diminished noise interference. This is a direct result of implanting spatially secure electrodes within the cortex, thereby reducing tissue interference between the electrodes and the neurons.^[3] Due to the spatial ambiguity and time lags often associated with ECoG readings, a wide sampling of the cortex should be analyzed



Mian Wang is a Ph.D. candidate in Dr. Thomas J. Webster's Nanomedicine laboratory at Northeastern University. His interest in biomedical engineering started at Shandong University where he obtained his bachelor's degree in Biotechnology. In 2013, he received his master's degree from George Washington University in DC. He then joined Northeastern University as a PhD student in Chemical Engineering as part of Professor Webster's group. His research interest focuses on kinds of biomedical applications of cold atmospheric plasma (CAP), especially on using CAP combined with nanoparticles for anti-tumor therapy.



Gujie Mi is a Ph.D. candidate in Dr. Thomas J. Webster's Nanomedicine laboratory at Northeastern University. His research focuses on the design of peptide-based and DNA-based self-assemble materials as artificial extracellular matrices to probe and modulate cell behaviors. Originally from China, Gujie received his Bachelor's degree in Pharmaceutical Engineering from East China University of Science and Technology. After graduation, he went on to pursue his master's degree in Pharmaceutical Sciences at Northeastern, working on the design and applications of rosette nanotubes to promote bone growth.



Thomas J. Webster, Ph.D., is the Art Zafropoulos Chair and Department Chair of Chemical Engineering at Northeastern University (Boston, MA, USA). He received his degrees from the University of Pittsburgh (B.S., Chemical Engineering, 1995) and Rensselaer Polytechnic Institute (M.S. and Ph.D. in Biomedical Engineering in 1997 and 2000, respectively). He pioneered the field of nanomedicine and was the first to discover increased tissue growth, inhibited infection, and decreased inflammation based solely on nanostructured features. His research had led to the formation of numerous companies and medical devices currently improving human lives.

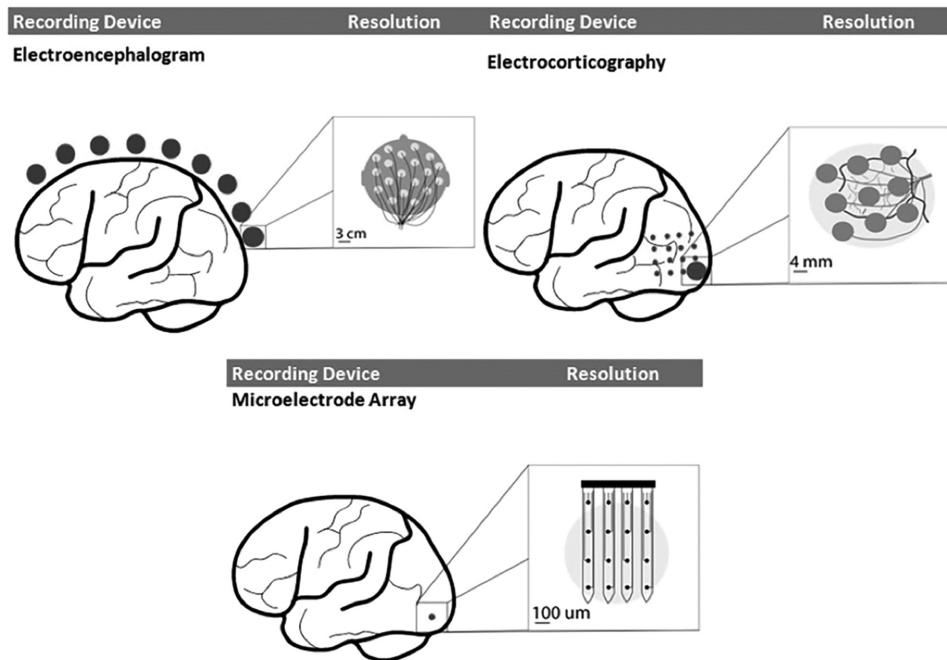


Figure 1. Electrophysiological and physical comparisons of neural recording systems.^[19] A comparison of the major electrode-based systems that are depicted, including EEG, ECoG, and microelectrode configurations, suggests a positive correlation between the degree of invasiveness of a device and the signal resolution that is achieved. However, this tradeoff may not be as significant with the current trend towards electrode miniaturization. Smaller probes can achieve cellular and subcellular resolutions while requiring less invasive implantation surgeries. Reproduced with permission.^[19] Copyright 2016, the authors.

over a fine temporal scale.^[20] Alternatively, a more invasive approach that targets neural assembly involves the measurement of local field potentials (LFPs). LFP signals are normally collected by microelectrodes that have higher impedance values than the larger electrodes used to obtain EEG data.^[3] By virtue, impedance is a common metric that is used to measure the performance of an electrode. The effective impedance of a probe is calculated by taking the summation of the impedances that result from 1) the resistance of an electrode material, 2) the resistance of the electrolyte, and 3) the capacitance and resistance at the electrode/electrolyte interface. Microelectrode design entails the optimization of several parameters, including the impedance. In general, a lower impedance value is associated with a higher recording quality. Despite the higher impedance values of microelectrodes, however, structural specificity, determined by relative neural placement, allows LFPs to measure localized electrical field fluctuations without requiring spatial averaging of bioelectrical activity (as is the case with EEG and ECoG). Even more invasive is the application of microelectrode arrays localized around the neuronal cell body. A neural action potential elicits a pulse or spike from the electrodes. These spike trains are characterized by extreme specificity, measuring the excitability of a single neuron.^[3,21] The drawback of this is an incoherent sampling of the complete neural population. Brain complexity inevitably contributes to a limited understanding of neural population dynamics. A principled neuroscience and engineering approach that integrates time-dependencies, quantification strategies, and materials research becomes necessary to design a device that is biocompatible, minimally invasive, and functionally feasible.

2.2. Design Considerations

The electrical infrastructure of an interface must be designed to process high signal-to-noise ratios (SNRs), while bypassing cell damage and extending BMI durability.^[3] Metal electrodes are often associated with a relatively poor SNR due to the incidence of thermal, or Johnson noise, that arises from electrode/electrolyte impedance at the implant site.^[22,23] Johnson noise is the thermal agitation of electrons inside of a resistor, which invokes random voltage fluctuations. This problem is associated with the difficulty of translating the ionic signals sent by neurons into electrical impulses within electrodes. Furthermore, poor mechanical stability at the tissue/electrode interface often leads to an observable discrepancy between the signals being recorded by the electrodes and the charges being delivered for neural stimulation. In principle, the charge injection capacity (CIC) at the tissue/electrode interface quantifies the charge being supplied by the electrodes to the neurons.^[23] For stimulation, it is desirable to apply small electrodes that can selectively trigger a targeted neuronal population. However, the onset of undesirable electrochemical reactions and inflammation can occur as a consequence of concentrated currents on small electrodes.^[23,24] Therefore, it becomes necessary to improve the efficiency of charge injection.

The biological response elicited by an implant material must be carefully considered during electrode fabrication. Due to the prolonged contact of invasive BMIs with neural tissue, neural interfaces must be engineered to withstand the physiological environment without posing any serious health risks to the user.^[3] Biological issues often arise due to the interruption

of blood-brain barrier operations and the onset of inflammatory and immune responses. Such reactions are associated with the influx of microglial and innate immune cells to the implant site, and consequential astroglia.^[3,25–28] Fibrous capsule formation may additionally isolate the implant and impair its function. In many cases, however, prolonged tissue–device contact is not even practical due to the mechanical mismatch disassociating rigid neural prosthetic device implants and native soft neural tissue.^[23] The most common metal- or silicon-based implants are a source for tissue straining and micromotion of electrodes within tissues. The effect of tissue straining at the implant site is in many cases an inflammatory response, with compromised stability at the metal/neural interface. In this case, inflammation has been associated with electrode failure that results because of the deposition of glial scars that encase the electrode and prohibit the transfer of neural signals.^[23,29]

To implement BMIs clinically, it is also necessary to consider functional specifications pertaining to power dissipation, scale, and computation. Ideally, differential amplifiers should sustain common-mode rejection ratios that approach infinity, in addition to high gains and nominal power dissipation.^[3] Minimizing power consumption prolongs the functionality of the control loop battery and helps evade battery replacement surgeries while sparing the neighboring biological tissue from sustaining heat damage.^[3,30] To provide a basis for comparison, current neural probe amplifiers and wireless implantable devices require 100 $\mu\text{W}/\text{channel}$ and 2.5–5.0 mW, respectively.^[3] Grid-computing is being examined as a viable approach for engineering extended lifetime BMIs.^[3] However, due to associated poor latency, or extended time-lapse intervals, that create an insulation barrier between direct signaling and feedback, real-time requirements pose an ancillary concern.

2.3. Current Trends in Biomaterial Neural Tissue Interface Design

Researchers have proposed a variety of modifications to address the challenges addressed above. For example, electrode coatings have included ceramic or other nano-structured matrices, conductive polymers, and/or drug eluting material conjugations.^[3,4,31] Organic-based bioelectronics are especially gaining attention due to their biocompatibility potential.^[23] Materials with lower Young's moduli have also been investigated to reduce mechanical mismatch. For example, parylene polymers and flexible polyamides, with Young's moduli of 2.8 GPa and 2.5 GPa, respectively, have been employed as substitutes for silicon or metal electrodes, despite having moduli that are still six orders of magnitude higher than that of brain tissue.^[31–35] More progressively, Capadona et al. have demonstrated that hydrated PVA-coated tunable cellulose nanocrystal (tCNC) composites, with a Young's modulus of 12 MPa (still significantly higher than the Young's modulus of the brain and other neural tissue), can be used to fabricate mechanically stable electrodes.^[36] For comparison, different brain regions are typically associated with Young's moduli of about 3–15 kPa, and individual cell types, including astrocytes and neurons, are reported to have nominal moduli, within the range 1–100 Pa.^[36]

Although soft and flexible neural prosthetic devices are difficult to insert surgically, PVA-coated tCNC is relatively stiff in the unhydrated state. Compared to silicon-based electrodes, tCNC electrodes demonstrate a 30–50% reduction in interfacial stress upon hydration and a reduction in inflammation of the surrounding tissue.^[36]

Alternatively, researchers have investigated microfluidic methods for guiding inflammatory or glial cell responses.^[3,4] For instance, micro-immunohistochemistry has been applied on 40- μm -thick rat brain thin-sections to determine the expression of glial fibrillary acidic protein (GFAP) in the region of implanted test electrodes.^[31] Other studies have sought to improve neuronal recording quality and capacity via the production of 3D electrode arrays.^[7] There are also efforts to limit heat damage to adjacent tissue during the application of complex and high-power assemblies by reducing the density of power being generated, which should not exceed 0.8 mW mm⁻².^[7,37] However, as previously mentioned, there are significant design challenges associated with wireless and/or dense multichannel electrode arrays which could limit the extent of circuit size reduction or power dissipation attenuation. The next section describes current fabrication technology in which nanotechnology is providing answers.

3. Technology for Electrode Fabrication

3.1. Micro-Fabrication Methods

A number of studies on the fabrication of microelectrodes have demonstrated the advantages of smaller electrodes and their benefits for neural applications.^[38–40] The benefits of micro-over macro-electrodes have been attributed to the rapid formation of radial diffusion fields and reduced Ohmic resistance, resulting in increased mass transport rates, enhanced current densities, and higher signal-to-noise ratios.^[41,42] These effects are suggested to be even more significant with the transition from micro- to ultramicro- (submicro- or nano-) electrodes, which will be discussed later.

3.1.1. Precision Fabrication

Precision mechanical fabrication has been a traditional method in the development of vagal nerve and deep brain stimulators, in addition to other electrode recording arrays that record current changes.^[43,44] Since most of the electrodes fabricated via precision fabrication are composed of metal, with thicknesses ranging from 10 μm to 100 μm , they typically have strong resistance to corrosion since they are passivated before use.^[45] Thus, electrode arrays made using this technology tend to have low corrosion rates and extended lifetimes in the biological environment. Precision fabrication has become widespread in the electrode fabrication industry due to low cost, commercial availability, and high customizability.^[46] However, challenges and limitations still exist with traditional precision fabrication. For example, it does not allow for the production of multi-layered devices containing insulation layers.^[47] In other words, the integration of an equal density substrate is required. In

addition, the manufacturing accuracy depends on the skills of the manufacturing technician, which limits device complexity. To overcome these drawbacks and achieve a better neural interface, one research group developed a new corrugated polyimide-based micro-electrode for use with intrafascicular peripheral nerves via precision fabrication.^[48] This corrugated design was achieved through tempering the polyimide substrate within a moldform. This fabricated electrode exhibited improved mechanical properties and load-displacement.

3.1.2. Laser Structuring

Laser structuring has been developed to overcome the drawbacks associated with precision fabrication.^[49–51] It allows for the quick and customized fabrication of electrode arrays with rationally designed shapes.^[52] Generally, electrodes are first designed by standard design software, such as AutoCAD. The design can then be directly transferred to various medical grade materials, including silicone rubber, alloys, and platinum foil.^[52,53] Contact pads and interconnect lines are usually embedded into silicone rubber sheets to achieve mechanical support and electrical insulation. The silicone rubber layer, which can be as thin as 25 μm , is fabricated by spin-coating

n-heptane diluted silicone rubber.^[54] A laser is then used to structure the silicone rubber-metal sheet-rubber sandwich based on the AutoCAD design. The entire fabrication process is shown and described in **Figure 2A**. Electrodes fabricated in such a manner have high mechanical stability imparted by the silicone rubber or by polymer foil coatings^[55] and sufficient flexibility is achieved by creating intricate zigzag-shaped electrodes.^[51,56] The lasers used for this technology have advanced considerably from nano- and picosecond lasers to the latest femtosecond lasers, which achieve shorter pulses and thus better resolution.

One of the conventionally used nanosecond Nd:YAG laser systems, with a wavelength from 1064 nm to 532 nm and pulse of 7–8 ns in duration, allows for the fabrication of micrometer-scale devices with feature sizes as low as 80–100 μm .^[52] However, when nanosecond or longer pulsed lasers are used to structure materials, melting of the treated region can result in unwanted recasting along material surfaces and edges. As a result, the fine control that is critical in electrode fabrication is hard to achieve. Recently, studies have shown that picosecond laser systems allow for the fabrication of feature sizes at least 3 times smaller than those achieved via nanosecond laser structuring,^[50] and femtosecond laser systems with shorter pulse duration times offer even better resolution than picosecond

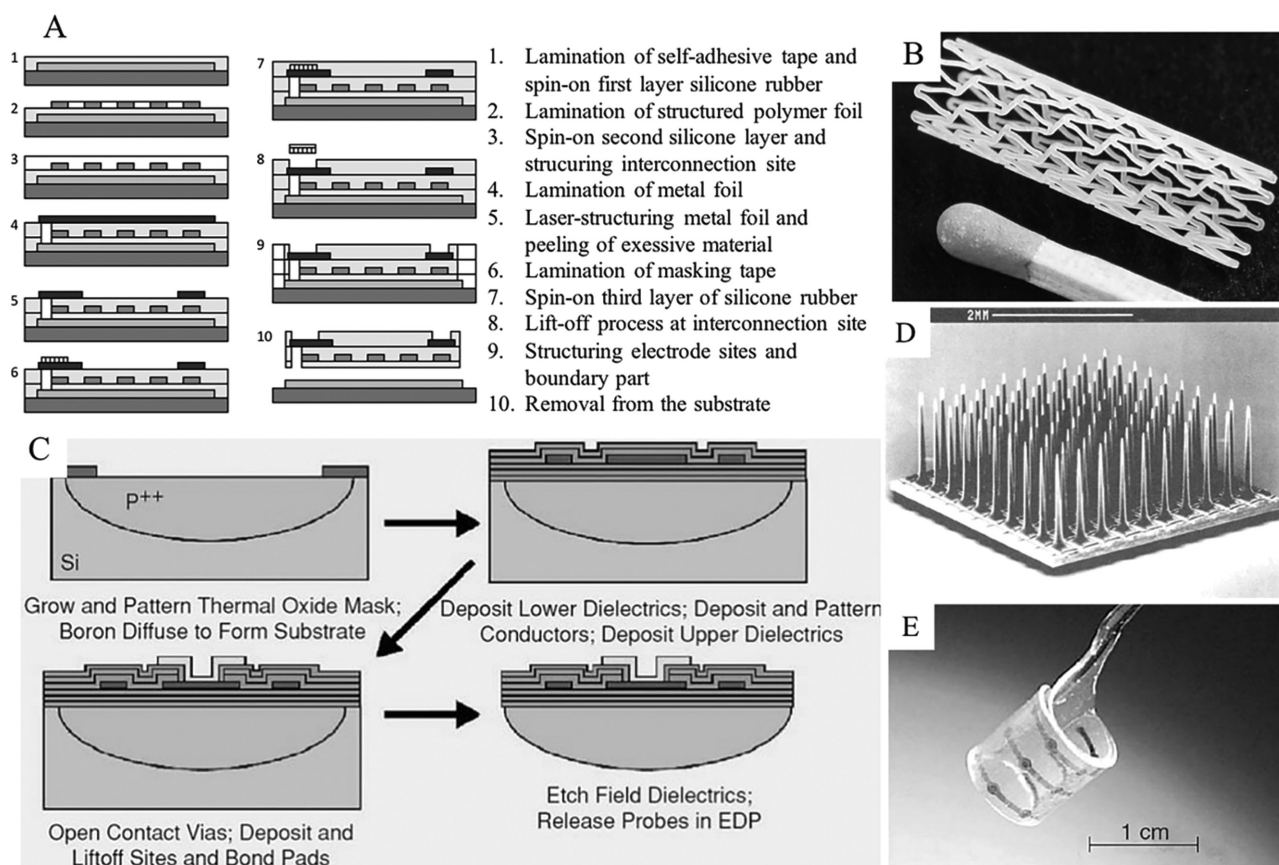


Figure 2. A) Cross-section schematic of the laser structuring fabrication process. Reproduced with permission.^[52] Copyright 2005, IOP Publishing. B) A medical stent micromachined from a biodegradable polymer using a femtosecond laser. Reproduced with permission.^[57] Copyright 2003, Scientific Research. C) A simplified fabrication process for the Michigan electrode assay. D) The Utah Array structure.^[64] E) Flexible polyimide-based electrode array. C–E) Reproduced with permission.^[64] Copyright 2010, Springer.

systems. Compared to nanosecond or picosecond laser systems, femtosecond lasers have relatively shorter pulse durations and higher repetition rates, which play an important role in processing extremely high quality parts^[57] (Figure 2B). As the pulse width decreases from nanoseconds to picoseconds to femtoseconds, the interaction time between the laser pulse and the substrate decreases, which allows for better resolution. An additional advantage of femtosecond lasers is their ability to micromachine a wide variety of substrates, including metals, glasses, diamonds, silica, polymers, and ceramics.^[58–60] However, results have demonstrated that femtosecond laser structuring might lead to debris formation, which could affect electrode precision. To avoid this issue, numerous studies have implemented ultrasonic wave liquid-assisted hole drilling processes. It was demonstrated that the incorporation of this technique significantly reduced debris generation and led to the formation of more precise edges.^[61–63]

3.1.3. Silicon-Based Neural Electrode Fabrication

With the development of lithographical techniques, microelectrodes made of semiconductors, such as silicon, have been introduced.^[64] Silicon-based electrodes with multiple electrode contacts can be fabricated via planar photolithographic complementary metal-oxide-transistor (CMOS)-compatible techniques on silicon wafers. Electrodes produced in such a way often have highly precise tip structures.^[65] One of the most common examples of silicon-based electrodes is the Michigan array, which combines several microelectrode sites into one array with the aim of achieving a higher density of sensors for implantation. The fabrication method can generally be broken into a few steps: first, patterned conductors are sandwiched by two layers of dielectrics before being deposited on a deep boron diffusion-defined probe shank. This is followed by a lift-off process that exposes the titanium or iridium electrode sites. Finally, silicon wafers are dissolved via isotropic wet etching and ethylene diamine pyrocatechol (EDP) etching processes (Figure 2C).^[64] During the 1970s, new technologies, such as microelectromechanical systems (MEMS), vapor deposition, and chemical etching were developed and applied to refine the fabrication of Michigan arrays.^[66] Design changes in the fabrication process, such as refined probe geometries and the integration of CMOS electronics, then began to earn credibility. Meanwhile, discrete insulated wires were replaced by flexible silicon ribbon cables, which provide better connection and better stability for long-term implantation.^[67]

The next developmental aim was to advance electrode arrays from 2D to 3D, which resemble freestanding high-aspect ratio microneedle structures with the electrical contacts located at the tip end.^[68] The electrodes are then sealed with rubber or glass, as shown in Figure 2E. The Utah array is an example of a 3D microelectrode array applied to neural interfaces. This 3D electrode array consists of 100 conductive lance-shaped silicon needles. Each of the needles is isolated and coated with platinum. The fabrication of the Utah arrays involves a multi-step process in which a p+ doped silicon wafer is subjected to molecular thermo-migration that yields p+ silicon trails along the wafer. After electrical isolation of

the p+ trails, the silicon wafer is micromachined to minimize the n-type silicon surface coating, which engenders a p+ trail sharpening. A thin layer of platinum is deposited on each tip, and electrical contacts are enabled through the incorporation of gold wires. These arrays have been successfully implanted in the cat auditory cortex and have been used for recording parietal cortex activity.

Many recent studies have also proposed the design of a fully implantable Utah array that features wireless connectivity.^[69] In these designs, miniature power supplies and telemetry systems are fabricated on the back of the electrode arrays, opening the possibility for full systemic implantation onto the cortex. Another study concerning a wireless electrode integrated a 100-channel Utah electrode array (UEA) (Figure 2D), a custom-designed IC with data processing, RF transmitter, power recovery, and SMD capacitors via UEA as a circuit board for the electrical connections. The study showed that the integration process they developed resulted in potentially good biocompatibility, well developed properties for advanced electrical and mechanical integration, and off-body control.^[70] This wireless UEA has the potential to be a platform technology for high-density integration of implantable microdevices and microelectronics with external control.

3.1.4. Other Micro-Fabrication Methods

Other microelectrode fabrication methods exist to meet the requirements for processing different materials. For example, one of the commonly used categories of materials in fabricating neural electrodes are metals, which is commonly molded into a stiff cone and embedded in glasses or polymers. In this case, the metal tip is exposed at the end of the electrode and serves as an electrode-tissue contact for recording current changes. The choice of metal can include gold, platinum, titanium, tungsten, or others, all of which exhibit high Young's moduli. Consequently, there is a huge mismatch in stiffness between the native brain tissue and metal-based electrodes. Flexible arrays have thus been developed to alleviate this issue and have been widely used in neural recording and stimulation applications.^[64] These flexible arrays can be fabricated by embedding one or more layers of a thin metal into polyimides that isolate and support the metal electrodes (Figure 2E). Then, dry etch processes are used to expose the contact points of the electrodes, and finally, the flexible electrodes are isolated by dissolving the silicon substrate. The following section describes how these now traditional methods can be improved through the use of nanotechnology.

3.2. Nanofabrication Methods

3.2.1. Nanofabrication Methods

Nanoelectrodes can be defined as electrodes with a critical dimension between 1 to 100 nm, where the critical dimension is mainly controlled by nanofabrication methods. The primary reason for the use of nanoelectrodes is the benefit obtained from enhanced mass transport and the increased Faradaic to

charging current ratio.^[71] As electrodes decrease in size from micro to nano, radial diffusion becomes more dominant, which can result in both faster and enhanced mass transport for diffusion-controlled Faradaic currents. In addition, the use of nanoelectrodes greatly improves the spatial resolution of neural stimulation, which represents a huge improvement over microelectrodes that often suffer from limited resolution.^[42] Lastly, the miniaturization of the active regions makes it possible to pack more nanoelectrodes with distinct functions into a multiplex device, which provides huge potential for the realization of massively parallel measurements. Despite their benefits, nanoelectrodes have not been as widely used as microelectrodes, primarily due to the lack of fabrication techniques for electrode miniaturization. In this section, four main fabrication methods, including electron-beam lithography, electrochemical methods, and nanomaterial based electrode fabrication will be discussed.

3.2.2. Electron-Beam Lithography (EBL)

Electron-beam lithography (EBL) involves the use of a finely focused beam to produce well-defined nanoelectrodes.^[72,73] As a short electron wavelength is typically used, which effectively avoids issues associated with diffraction, EBL fabrication has the potential to achieve extremely high resolution down to the nanometer range.^[74] The main purpose of lithography is to create a designed pattern in the resist layer, which can be further transferred onto an underlying substrate. Compared with electrochemical plating, shadow evaporation, and other methods, which involve a series of complicated processes, EBL technology offers the advantages of ultra-micro size, low cost, reproducibility, and high reliability.^[71] EBL can also be used with a wide spectrum of materials.^[75]

Based on the different processes involved, EBL writing techniques can be divided into two distinct schemes: direct writing and projection printing.^[76] In direct writing, a designed wafer is exposed to a focused narrow beam of electrons. Alternatively, in projection printing a large-sized e-beam pattern is projected in parallel through a mask onto the photoresist substrate, which results in an embossed nanoelectrode pattern.^[72] For both methods, the energy of the e-beam to which the substrate is exposed plays an important role in the fabrication process. It was found that a better resolution can be achieved when high energy electrons are directed onto the substrate (between 50–100 keV).^[77] However, backscattered electrons generated by high-energy electron beams will lead to the exposure of neighboring areas to these rebounded electrons, a phenomenon referred to as the proximity effect. The proximity effect is often associated with a loss of resolution. One possible strategy to overcome this response is to operate EBL at a low energy state (between 2–20 keV).^[72] While effectively preventing the proximity effect, the penetration depth is limited as most of electrons will use up their energy in the resist layer before reaching the substrate. Thus, this approach achieves high resolution at the expense of cost and productivity.^[73] Alternatively, researchers have started to focus on improving resist technology rather than manipulating e-beam energy. An ideal resist material should have high contrast, high sensitivity, high

plasma etching resistance for pattern transfer, and small molecule size.^[78,79] Additionally, to achieve a high resolution while minimizing the electron scattering, a thin resist layer is highly preferred.

3.2.3. Electrochemical Methods

Ever since the early work on polypyrrole (PPy)/PSS coated neural probes pioneered by Cui and co-workers,^[80] electrochemical polymerization has been the preferred and most common method of fabricating conducting polymer (CP) coatings on neural electrodes, since it allows for direct formation of thin-layer polymer coatings on the electrode site. These coatings are typically characterized by low impedance and good adhesion, and can have nanoscale dimensions. The amount of material deposited (i.e., thickness of the film) and roughness of the film can be precisely and reproducibly controlled by varying the deposition time^[81] or the total charge passing through the system.^[80] Further studies have been conducted by several researchers to use conductive polymers doped with carbon nanotubes (CNTs) or graphene via electrochemical polymerization (Figure 3A,C).^[82–85] Electrochemical polymerization is typically carried out using a three-electrode configuration in a solution containing a monomer, solvent, and electrolytes (such as dopants and biologically relevant molecules). Doping and entrapment of molecules within the CP occur simultaneously, thus eliminating the need for post-synthesis modification. For instance, PEDOT and CNTs were electrochemically deposited onto Pt microelectrodes by Luo et al. to create nanostructured surfaces on microelectrodes (Figure 3B).^[83] The PEDOT/CNT film constituents were electrodeposited via a traditional three-electrode configuration with Pt microelectrodes acting as the working electrode, silver/silver chloride (Ag/AgCl) as the reference electrode, and a platinum wire as the counter electrode. Further in vitro studies demonstrated that this PEDOT/CNT-coated electrode had lower impedance. It was also found that the electrode was nontoxic and could support the growth of neurons.

In addition to CPs, metals or alloys are also widely used to fabricate neural electrodes via electrochemical deposition. In a recent study, Wang et al. elegantly demonstrated that ZnO/CdTe core-shell nanocable arrays can be vertically aligned on indium tin oxide (ITO) via an electrochemical deposition process,^[86] in which the CdTe layer was electrodeposited from an aqueous solution of potassium tellurite and cadmium acetate (Figure 3H,I). The resulting nanocable array was shown to have promising photoelectrochemical properties, which can be useful in light sensor or solar energy conversion. In another study, copper was electrodeposited onto a CNT wafer to create a multi-tiered current pathway, which was further shown to exhibit relatively high ampacity compared to the pure metal.^[87] In this fabrication scheme, shown in Figure 3E–G, CNT wafers were lithographically patterned into specialized configurations, and then copper was electrodeposited from an organic electrolyte solution into the pores of the CNT film. Finally, a nanostructured surface was created on CNT-Cu composites, as shown in Figure 3G. In addition to providing better electrical conductivity, this technique improved thermal stability by more than

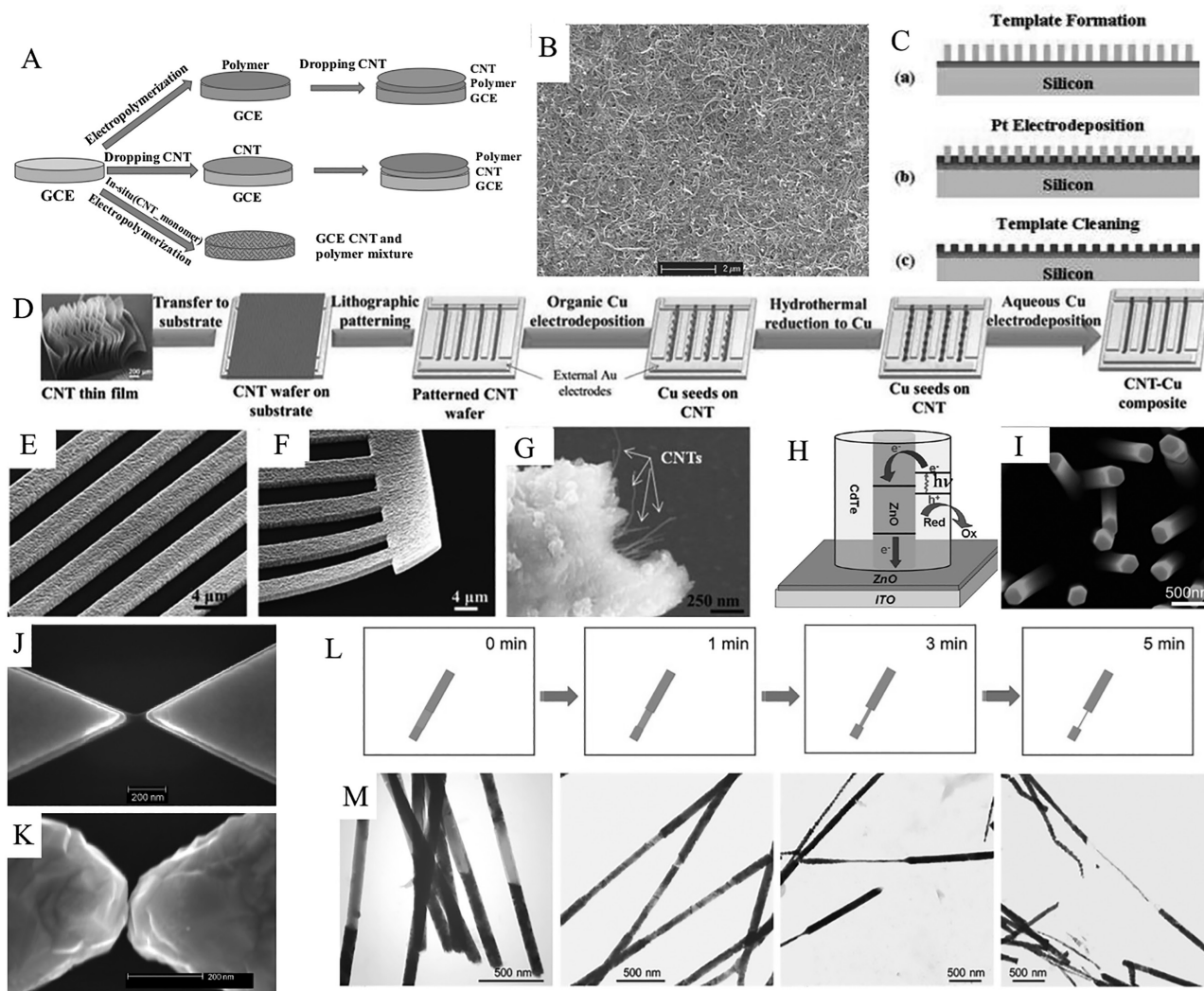


Figure 3. A) Schematic illustration for the fabrication of CNT-CP composite electrodes. Reproduced with permission.^[95] Copyright 2010, Elsevier. B) SEM images of CNT coated on an electrode surface. Reproduced with permission.^[83] Copyright 2011, Elsevier. C) Schematic of the fabrication procedures for a non-enzymatic glucose micro-sensor with nanoporous Pt on a silicon substrate. Reproduced with permission.^[89] Copyright 2008, MDPI. D) Schematic of a fabrication to develop sub-micrometer features on the CNT-Cu composite. E, F) SEM images of a CNT-Cu composite. G) SEM images of a fractured cross-sectional surface of the CNT-Cu composite. Reproduced with permission.^[87] Copyright 2015, Royal Society of Chemistry. H, I) ZnO/CdTe core-shell nanocable arrays can be vertically aligned on indium tin oxide (ITO) via an electrochemical deposition process.^[86] Reproduced with permission.^[86] Copyright 2010, American Chemical Society. J, K) Gap narrowing by electrodeposition. Reproduced with permission.^[94] Copyright 2008, American Chemical Society. L) Schematic of the etching time effect on penetration length.^[93] M) TEM images of nanowires after dipping them into a copper-citrate electrolyte and subsequently etching them in boric acid-citrate electrolyte for 1, 3, and 5 min. Reproduced with permission.^[93] Copyright 2016, American Chemical Society.

10 times in comparison to pure copper, something which could prove to be useful for the future development of efficient electrical devices or implantable electrodes.

In some cases, the electrochemical method is not directly used for the fabrication of electrodes, but rather as an important assistance step.^[88,89] One promising study was carried out by Lee et al. who used electroplating to fabricate nanoporous Pt electrodes on silicon substrates.^[89] This process was conducted using a three-electrode system consisting of a Pt bar, an Ag/AgCl electrode, and 3 mol L⁻¹ NaCl as the reference electrode. The porous Pt electrode template was then dissolved and cleaned, resulting in a nano-featured silicon electrode. Further studies demonstrated that one class of sensitive electrodes

can be achieved by narrowing the air gap separating the two electrodes. Chemical narrowing,^[90] electromigration induced break-junction,^[91] and template-assisted electrodeposition displacement,^[92,93] are possible techniques for minimizing this gap to the nanometer scale. For example, Shi et al. proposed a novel mode of electrochemical nanofabrication that produced a nanogap of around 100 nm via atom-scale junction formation.^[94] More recent studies by Geng et al. demonstrated the use of template-assisted electrodeposition of Fe-based alloy nanowires to create a thin nanowire segment via electrode-displacement with noble ions like Cu(II).^[93] The displacement layer was embedded between two Fe-No-Co layers, and the de-alloyed penetration length was carefully controlled in order to

form nanowire segments. A general Tafel model that relates with etching time of the displacement reaction with copper ions and the de-alloying corrosion reaction with protons was developed and used to predict the effect of these parameters on penetration length. It was found that a proton-to-copper ratio of 0.5 provided the longest etching time, which eventually led to the smallest diameter (less than 30 nm) of nanowire segments (Figure 3L,M). Nanowires prepared by electrochemical etching can therefore be very promising in fabricating electrodes that require higher sensitivity, such as those used for molecular sensing applications.

3.2.4. Nanomaterial-Based Electrode Fabrication

One of the most commonly used nanomaterials for fabricating nanoelectrodes are carbon-based materials.^[96–98] To create nanosurfaces on conventional electrodes, CNTs were coated on different substances, such as stainless steel,^[98] tungsten wire,^[98] glassy electrode,^[99] and copper electrodes^[100] via four different methods: deposition from aqueous solution, chemical vapor deposition (CVD),^[101] electrochemical deposition,^[97] and polymerization.^[98] Gabay et al. directly synthesized CNTs on p-type silicon microelectrodes with a Ni catalyst layer via chemical vapor deposition at 900°C.^[97] Dense and intertwined CNT meshes grown over the microelectrode surface resulted in a large drop in impedance. Well-resolved spikes with exceptional signal-to-noise characteristics were observed from rat cortical neuron recordings.

Similarly, graphene was also used as a nanomaterial in nanoelectrode fabrication. Hess et al. prepared graphene by chemical vapor deposition (CVD) and transferred the material onto sapphire substrates. This resulted in a graphene-based, solution-gated field-effect transistor (G-SGFET).^[102] This study revealed that graphene-based transistors have low noise and large transconductive sensitivity (Figure 4A,B). However, this CVD manufacturing process has its limitations within a high temperature environment, and Ni catalyst layer deposition can be a challenging task.^[103] This is a significant issue since most coating processes, including covalent bonding, electropolymerization, and electrochemical deposition are typically conducted at room temperature.^[104] The history of electrochemical deposition can be traced back to as early as 1985, when Gross and his co-workers tried electrochemical deposition of an aqueous suspension of multi-walled CNTs (MWCNTs) on indium-tin oxide multi-electrode array (MEA) electrodes^[105] (Figure 4C). The CNT coatings displayed a rice-like morphology on the electrode surfaces. Measurements showed that the impedance significantly decreased and charge transfer increased more than 40-fold when compared with uncoated samples.

In order to distinguish these different fabrication methods, Keefer et al. compared three coating methods (aqueous deposition, electrochemical deposition, and electropolymerization) with their effect on electrode–tissue interfaces both in vitro and in vivo.^[98] CNTs were first deposited via direct deposition from an aqueous solution (0.3–3 mg mL⁻¹) of MWNTs, which can be flanked by a thin CNT surface layer; however, results were not ideal because this method cannot form uniformly and strong banded CNT layers.^[98] On the other hand, electrochemical

deposition was used to covalently attach acid-chloride-functionalized CNTs to amine-modified electrode surfaces under constant voltage conditions, at 10 V for 70–90 min. In addition, carboxyl-modified CNTs were polymerized onto conductive polymers under a 0.75 V applied voltage. Both of these methods were very efficient at depositing CNTs that would yield neural electrodes with enhanced conductivities. In addition, He et al. also deposited SWNTs on gold substances via photopolymerization.^[106] A monolayer cys-PEGDA was synthesized on the gold electrode surface, and then the functionalized SWNTs were purified and carboxylated by sonication in a mixture of sulfuric acid and nitric acid (3:1, v/v). Results of photopolymerization on Au-Cys-PEGDA surfaces under UV light exposure ($\lambda = 365$ nm) (Figure 4D) indicated that the hybrid hydrogel possessed good electrochemical performance. In particular, the charge transfer was quasi-reversible and diffusion-controlled, and R_{ct} dramatically decreased from 428 000 Ω for pure hydrogels to 42, 70 Ω for hybrid hydrogels. In addition, PC12 neural cells adhered well to the coating, which implied that the covalently bonded coating offered good biocompatibility to neural tissues. More recent work reported by Nicolas et al. used electropolymerization to coat MWCNTs on folating microelectrode arrays (FMAs).^[107] During this process, a potentiostat with a platinum counter and Ag/AgCl reference electrodes were used to apply a constant 1.3 V coating potential for 30 s. SEM images showed an open CNT layer with nanofibrous morphology on the microelectrode surface (Figure 4E). This coated electrode decreased impedance in vivo and showed no disturbance to neural activity upon CV stimulation.

Another widely used material in nanoelectrode fabrication is CP (Figure 4F). CPs can be fabricated by either chemical or electrochemical polymerization, which each carry their own set of advantages and disadvantages.^[108,109] Although oxidative chemical polymerization enables the synthesis of highly ordered structures and the possibility of larger scale production as well as post-covalent modifications, the synthesis is more complicated, and the resulting polymers often suffer from poor electrical conductivity. These polymers are often doped post-synthesis.^[110] Additionally, sophisticated patterning techniques, such as nanoimprint lithography^[111] and hierarchical patterning,^[112] are often required post-chemical polymerization to incorporate large-area nanoscale patterns. In cases when a biomolecule is used as the dopant to improve biocompatibility, chemical polymerization is not a viable approach because many of these biological molecules are not compatible with the redox chemistry that is required for chemical synthesis.^[113,114] In contrast, electrochemical polymerization has been preferred and is a more common method for fabricating CP coatings on neural electrodes as it allows for direct formation of thin-layer polymer coatings on the electrode site down to the nanoscale^[115] with low impedance and good adhesion.^[116] Doping and entrapment of molecules within CPs via electrochemical polymerization is happening simultaneously without the need for post-synthesis processing.^[117] In addition, the physical and electrical properties of the resulting polymer can be manipulated in a simple one-step process by altering the polymerization conditions, including the pH, temperature, applied voltage and choice of dopant, which would enable a superior device for neural interfacing applications.^[118]

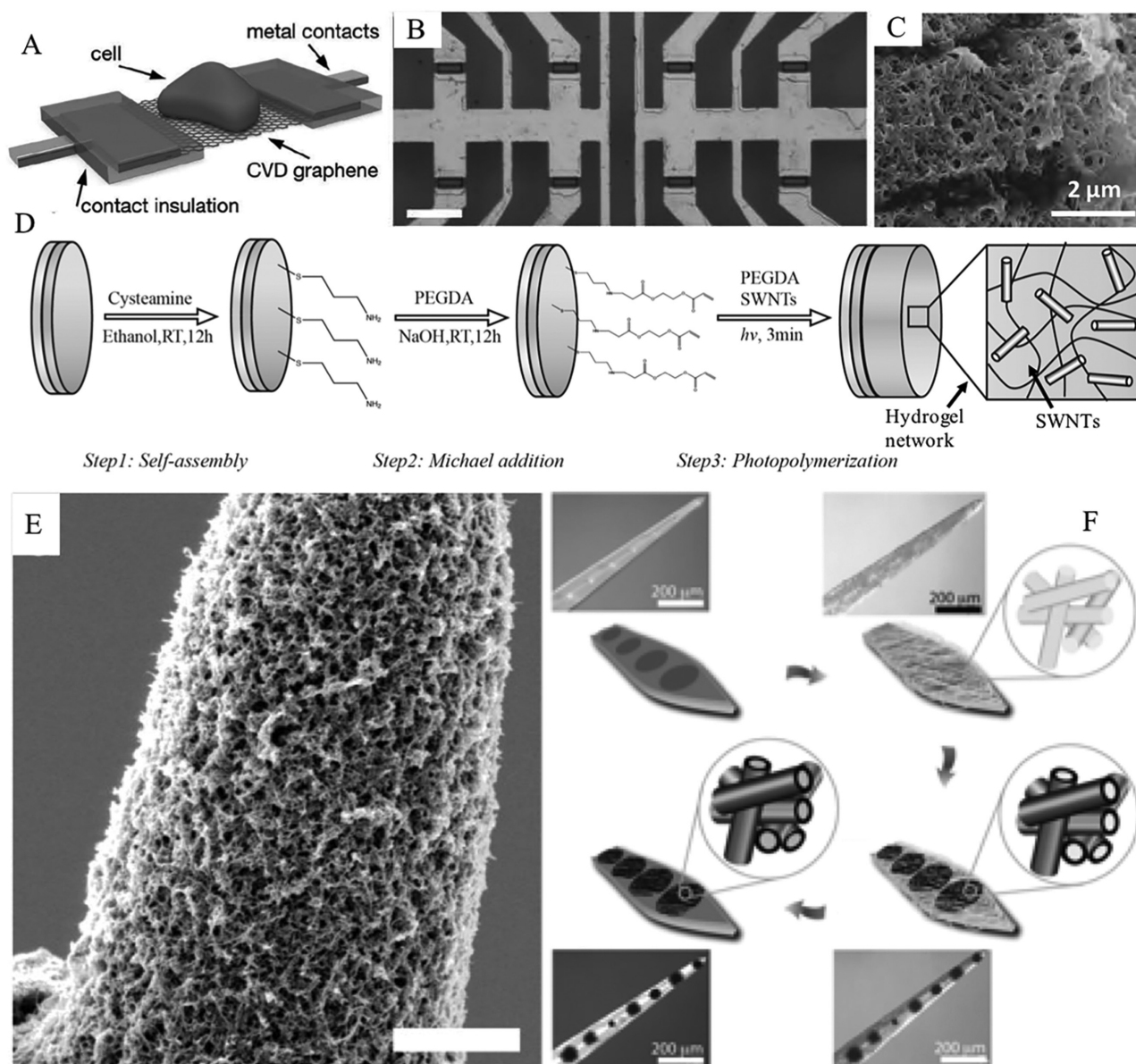


Figure 4. A) Schematic view of a CVD graphene sheet with a cell on the gate area;^[102] B) Optical microscopy image showing eight transistors in the central area of a CVD graphene sheet (Scale bar = 50 μm). Reproduced with permission.^[102] Copyright 2011, Wiley; C) SEM images of MWCNTs on indium-tin oxide multi-electrode array (MEA) electrodes. Reprinted with permission.^[211] Copyright 2011, IOP Publishing. D) Fabrication of photopolymerization of a hybrid hydrogel coating on a gold electrode surface. Reproduced with permission.^[106] Copyright 2011, Elsevier. E) SEM images of a CNT layer with nanofibrous morphology on the microelectrode surface (Scale bar = 3 μm). Reproduced with permission.^[107] Copyright 2008, MDPI. F) Schematic illustration of CP nanotube fabrication on neural electrodes: deposit biodegradable polymer, such as PLLA onto the electrodes, coated with CP via electrochemical deposition, and dissolve the core fiber, then CP nanotubes are formed. Reproduced with permission.^[216] Copyright 2010, Wiley.

3.3. Electrode Evaluation and Characterization

Two primary charge-injection mechanisms have been proposed at the electrode–tissue interface, capacitive reaction or Faradaic reaction. Capacitive reactions only involve the charging and discharging of the electrode–electrolyte double layer and can be further subcategorized into electrostatic or electrolytic reactions. On the other hand, other than capacitive charge-injection in which no electron is transferred between the electrode and electrolytes, Faradaic charge-injection involves oxidation or reduction of

chemical species on the surface of the electrode or in solution and therefore has electron transfer between the electrodes and electrolytes.^[119,120] Since products formed by Faradaic charge injection cannot be recovered by reversing the current, chemical species generated and/or consumed during the stimulation pulse may result in irreversible, toxic interactions with the surrounding tissue. As a consequence, a Faradaic reaction sometimes is less desirable than a capacitive charge-injection process.^[121]

There are certain criteria when selecting materials as implanted electrodes and those standards are mainly based on

the assessment of biocompatibility and tissue-electrode impedance at 1 kHz, a biologically relevant frequency within the range of neural cell communication frequencies.^[122] First and foremost, materials used for fabricating electrodes must be biocompatible with limited toxic effects to the surrounding tissue, and should minimize foreign body or immune responses. In order to reduce a tissue response, such as encapsulation of electrodes or necrosis, numerous studies have been carried out by different groups. The overall results summarized by Agnew and McCreery^[123] suggested that metals including silver, copper, nickel, magnesium, zinc and cobalt would induce severe toxicity and an allergic response to local tissue while aluminum, platinum, titanium and CPs (like PEDOT) have much better biocompatibility towards surrounding tissues.^[124–127] In addition to the materials themselves, it is required that chemical species generated by Faradaic reactions during the electrical stimulation should not be toxic to local tissue. Second, materials should be able to maintain their integrity during and after the surgery if it is for a long-term usage. There should not be any movement between the implanted device and surrounding tissue after the surgery and the electrode needs to remain stable within the intended duration of use.^[121] Finally, in order to elicit action potentials from neuron cells, a sufficient magnitude of charges needs to be delivered in a pulse paradigm by the electrode. In the meantime, however, the charge per electrode surface area has to be controlled below the maximum surface charge density of a material to minimize any electrochemical reactions occurring on the electrode surface. Therefore, in addition to size reduction, decreasing electrode impedance and enlarging charge-injection capacity are the top concerns to improve the operational lifetime of implanted electrodes.^[128,129] Consisting of two components, resistance and reactance, impedance is a general circuit parameter that highly depends on the species, surface area and surface roughness of an electrode–electrolyte interface.^[130] Since simply increasing surface area by increasing geometric size would have a negative effect on in vivo applications, manipulating material morphologies, such as increasing surface roughness, becomes a great strategy to increase effective surface area without changing electrode size. Some recent studies demonstrated that by coating PEDOT or CNTs onto electrode sites and forming fibrils or films, effective surface area of the electrode was significantly increased and impedance was decreased as a corresponding result.^[71,127]

To characterize and assess neural electrode electrochemical behavior, cyclic voltammetry (CV), impedance spectroscopy and potential/voltage transient measurements have been applied both in vivo and in vitro. CV is a type of potential-dynamic electrochemical measurement that can identify the electrochemical properties of analytes and provide information on the thermodynamics, kinetics, reversibility and stability of the electrochemical reactions on the electrode. In cyclic voltammetry, three types of electrodes, a test/working electrode, a counter/auxiliary electrode and a reference electrode, are used to measure the potential. The working electrode is the electrode that is under investigated. The counter electrode is employed as a sink so that the current can flow from the external circuit to the site. Reference electrodes, in many cases Ag/AgCl or Hg/HgCl/KCl, are electrodes that are stable and have a well-measured electrode potential. Generally, a cyclic voltammogram is

plotted by detecting the current from the working electrode during the sweep. More importantly, as reported by Negi et al., the CV response changes with different sweep rates, electrode surface area and roughness, regardless of whether that electrochemical reaction remains stable.^[131] In a study, a sputtered iridium oxide film (SIROF) was compared with activated iridium oxide film (AIROF) concerning aspects of surface morphology, impedance and charge capacity, and results from CV indicated that SIROF had significantly higher internal area than AIROF, which resulted in higher charge storage capacity (CSC).

Another electrode characterization method being used is impedance spectroscopy. With electrochemical impedance spectroscopy (EIS), impedance and phase angle are obtained by first applying a small sinusoidal potential with a fixed frequency, and then repeatedly measuring and computing the generated impedance at each frequency which is usually between 1 Hz to 10⁵ Hz.^[118] Since information obtained from EIS is significantly more than single frequency measurements, this technique can not only be used to investigate the recording capabilities of electrodes and electron transfer rate of reaction, but also can be useful in estimating the influence of tissue conductivity to the overall electrode impedance. The last approach for electrode characterization is voltage/potential transient measurements, which is frequently used to estimate the maximum charge-injection capacity and maximum positive and negative polarization under a controlled current/voltage. Similar to CV, a noncurrent-carrying reference electrode can be employed in this method as well. The resulting curve of voltage transients of the working electrode vs reference electrode during long-term pulsing will indicate whether the electrode is stable and safe to use.^[118] Although the voltage transient measurement is one of the commonly used approaches to detect charge-injection thresholds, additional concerns and limitations appears as well. For instance, as indicated by Cogan et al., current density has to be measured as well since charge-injection capacity heavily relies on it. In addition, the charge-injection capability can only be an estimated value since the stimulating current is nonuniform and could cause an electrode potential to vary over the electrode surface.^[132]

4. Nanomaterials Used for Neural Electrodes

4.1. Overview of Nanomaterials used for Neural Electrodes

The application of nanotechnology to neuroscience is of great interest since signal processing of neurons always occurs below the micrometer level. In recent years, progress has been made with nanotechnology to form bioelectrical contact with live cells in the nervous system.^[103] Nanoelectrodes are electrodes with a critical dimension in the nanometer range, and can be further categorized into individual nanoelectrodes, nanoelectrode arrays (NEAs), or nanoelectrode ensembles (NEEs).^[133,134] Generally, nanoelectrodes are recognized by their length scale and critical dimensions that control the electrochemical response. Similar to microelectrodes, nanoscale electrodes are expected to reduce the size to a greater extent. Compared to conventional electrodes with a millimeter diameter range, the primary advantage of developing nanoscale electrodes is the enhancement of the mass

transport phenomenon with radial diffusion. This high speed mass diffusion due to electrode size reduction can bring about faster electrochemical reactions, since the electron transfer process is no longer limited by mass transport.^[135,136] As a result, nanoscale electrodes and interfaces offer unique benefits in numerous neural interface applications, including improving the sensitivity of neural interfaces, ability to execute single live-cell studies and/or the development of highly efficient personalized biosensors. In other electrochemical applications, the enhancement of reaction rates and amplification of bio-signals have also been demonstrated by different research groups.^[133,134]

However, critical technical challenges, such as the increase of impedance and Johnson noise, also arise with the size reduction of conventional electrodes. Since the Johnson noise, also known as thermal noise, is proportional to the square root of the resistance of the electrodes, metal/alloy electrodes with large impedance will have difficulty in obtaining relatively weak extracellular potentials from baseline noise.^[103] Meanwhile, long term stability is another critical factor that has to be considered in designing nanomaterials. As a consequence, sufficient mechanical strength and toughness have to be maintained after miniaturization without compromising the ability to transfer electrical charge between the electrode and the tissue.^[137] In this sense, classical metallic materials that have been used to fabricate neural electrodes may not remain applicable and new types of materials, such as conductive polymers and hybrid organic-inorganic nanomaterials, have begun to emerge as promising candidates for fabricating nanoelectrodes.^[138] All properties of these nanomaterials pertinent for neural applications can be found in **Table 1**.

4.2. Graphene

4.2.1. Overview of Graphene

To date, most implantable electrodes are composed of silicon and/or noble metals. Although these rigid materials meet most criteria and present good chemical stability, drawbacks such as inducing “glial scar” on the electrodes^[139] that eventually weaken the intensity of the desired signal (signal-to-noise ratio) impede their long-term biomedical applications. To address this obstacle, several attempts have been made to discover potential candidates that possess better electrical conductivity and stability in the biological environment. Among all proposed materials, carbon-based nanomaterials such as graphene and CNTs are believed to be excellent candidates as neural electrodes and have been intensively investigated owing to their unique chemical and electrical properties.^[140] Distinguished from the 3D structure of CNTs, graphene is formed by a single 2D layer of sp²-hybridized carbon atoms in a hexagonal arrangement,^[141] and this major structural difference leads to their improvement in many aspects, such as electronic biosensing.^[142]

4.2.2. Electrical Properties

Among all of graphene’s exceptional properties, including exceptional surface area and mechanical strength,^[143–145]

thermal and electrical conductivity,^[146] and high carrier/electron mobility,^[147] biomedical researchers have focused on their electrochemical properties. As one of the most promising candidates for neural engineering, graphene has been used as a complement for silicon and metal electrodes to develop novel neural interfaces and electrical recording devices with higher conductivity and lower toxicity.^[143,144] In a study by Perez et al. in 2015, graphene suspensions prepared by electrochemical exfoliation were combined with iridium oxide nanoparticles (IrOx-eG) to improve charge capacity and cell viability. Compared with pure IrOx coatings, this graphene-based coating enhanced neural stimulation frequencies without compromising cell compatibility and material stability.^[148] Another study reported by Chiu et al. also pointed out that graphene modified silver electrodes had less of a phase shift phenomenon in electrochemical impedance spectroscopy (EIS), which indicated a pronounced improvement in reducing electrode impedance.^[147] In addition, Li et al. stated that compared with bare carbon paste electrodes (CPE), graphene doped CPE exhibited a better performance with respect to electrocatalytic activity, mostly owing to the greater conductivity and larger surface area of graphene.^[149]

Apart from pure graphene, graphene derivatives, particularly graphene oxide (GO) and reduced graphene oxide (rGO), have also been applied in constructing neural interface composites. GO has been employed in a variety of fields such as electronic and imaging.^[150,151] For instance, a glassy carbon (GC) electrode was coated with a monolayer of a GO sheet and electrodeposited with Au nanoparticles, and the fabricated nanoelectrode ensembles (NEEs) were applied as DNA detection probes. As a result, the GO and Au modified NEE showed both higher sensitivity and better stability, and were able to detect as low as 0.5 amol DNA in a 5 μL solution. Another study also reported that wet-spun liquid crystal graphene oxide (LCGO) fiber brush electrodes exhibited high charge injection capacity and the ability to stimulate retinal ganglion cells.^[140]

However, due to their electrically insulating properties, other conducting materials such as conductive polymers and metals are usually combined with GO to fabricate electrodes. In addition, more recent studies have begun to raise concerns on its cytotoxicity towards different types of cells,^[152] mainly by inducing reactive oxygen species (ROS).^[153] As a result, rGO has emerged as a promising alternative for fabricating neural electrodes. Since a single layer of defect-free graphene is difficult to produce, the synthesis of graphene oxide followed by a chemical reduction of the oxygen group provides an alternative way to produce graphene-based nanomaterials with higher hydrophilicity (**Figure 5A,B**).^[154] Synthesized rGO or chemically converted graphene have been widely investigated by various groups. To better understand its electrochemistry properties, electron transfer studies on reduced graphene sheet films (rGSFs) were conducted and the synthesized graphene was examined with different redox species, including Ru(NH₃)₆^{3+/2+}, Fe(CN)₆^{3-/4-}, Fe^{3+/2+} and dopamine. By calculating electron-transfer rate constants (*k*⁰) from cyclic voltammetry (CV), Tang et al. demonstrated that the exceptional electronic structure of graphene enables faster electron transfer and therefore renders a significantly higher *k*⁰ value as compared to glassy carbon electrodes.^[155]

Table 1. Nanomaterials and their properties used for electrode fabrication.

	Materials	Electrical properties	Mechanical properties	Biocompatibility	References
Graphene	Pristine Graphene	Improved charge capacity and enhanced neural stimulation frequencies were found in vitro; reduced silver electrode impedance; increased signal-to-noise ratio.	High tensile strength and high stiffness.	Improved metal electrode biocompatibility in vitro; increased ROS levels and cytotoxicity at high concentrations in vitro.	[147,148,159,288]
	GO	Electrically insulating, usually combined with other metals to improve electrode sensitivity and stability.	High tensile strength and high stiffness.	Concentration dependent cytotoxicity.	[140,152,153]
	rGO	Enabled fast electron transfer; reduced glassy carbon electrodes impedance; reduced impedance values when compared to SWCNT in vitro.	High tensile strength and high stiffness.	Facilitated cell proliferation and neurite outgrowth on PC 12 cells; limited short-term toxic effect and non-significant neurotoxicity up to 7 days in vivo.	[155,156,163,171]
Carbon Nanotubes (CNTs)	SWCNT/PEGDA	Quasi-reversible, diffusion-controlled charge transfer. Charge transfer resistance decreased by order of magnitude.	Soft hydrogel reinforced by addition of SWCNTs.	Good attachment and growth of PC12 cells in vitro.	[289]
	PEDOT/MWCNT	Significant decrease in 1kHz impedance at early times. Increased charge storage capacity (study conducted in vivo).	–	Encapsulated within protein corona in vivo (rat visual cortex). Successful signal recording up to 11 days.	[107]
	Purified MWCNTs	Increased synaptic currents and action potentials measured by current clamp recordings in vitro.	–	Maintained cell adhesion and increased dendrite elongation of hippocampal neurons in vitro.	[194]
CPs	PPy/SWCNT	High safe charge injection limit, low 1 kHz impedance, good stability.	–	Good attachment and neurite outgrowth of PC12 cells in vitro. Significantly lower glial fibrillary acidic protein and higher neuronal nuclei immunostaining in rat cortex.	[213]
	CNT multi-electrode arrays	High surface and volume specific capacitance. Low and consistent impedance in range from 1 Hz to 20 kHz. High fidelity.	Flexible and durable.	Improved rat cortical cell attachment in vitro. Increased extracellular signals recorded.	[290]
	PEDOT nanotubes; PPy nanotubes	Impedance of neural electrode sites decreased and charge storage capacity increased compared to both bare iridium and CP films.	Less susceptible to delamination compared to PEDOT or PPy films	Cultured dorsal root ganglion explant remained more intact and exhibited longer neurites.	[291]
Hybrid materials	PPy/SWCNTs; PEDOT/CNTs	Higher safe injection limit; 95% reduction in impedance at 1 kHz; improved electrochemical stability; higher signal to noise ratio.	Improved mechanical stability.	Excellent biocompatibility and cell adhesion in vitro; decreased expression of GFAP and higher neuronal density in the vicinity of the implant in vivo.	[292,293]
	PPy/SG; Graphitic foliates/MWCNTs; GO/PEDOT	Improved both conductivity and electrochemical stability.	–	Exhibited minimal cytotoxicity and supported neuron growth with longer neurites.	[255,294,295]
	PVA/PAA; PEG/PU	Can suffer from a loss of electrical properties (exemplified by an increase in impedance and a decrease in charge storage density).	Tunable mechanical properties.	Higher neuron density, enhanced production of neurite extensions, significantly lowered GFAP levels and attenuated glial scarring.	[273,274]
	PPy/Alginate; PEDOT/Algin-ate; PEDOT/RGD-alginate; PNAI/heparin-methacrylate	Significantly lower impedance at 1 kHz both in vitro and in vivo; increased charge storage capacity; improved signal to noise ratio.	Have the potential to decrease elasticity down to the range of 1–10k Hz, which can provide additional mechanical buffer zone.	Non-cytotoxic to spiral ganglion neurons.	[281,282,287,296]
	CNT/GelMA	Excellent anisotropic electrical conductivity.	Elastic moduli of 1 mg/ml CNT/GelMA was 23 kPa.	Preserved high cell viability and supported cell adhesion.	[285]
	Graphene/PDMAA	Low impedance and high conductivity.	Compressive strength of the graphene/PDMAA was around 2.62 MPa; self-healing.	Good cellular attachment of PC-12 cells.	[286]

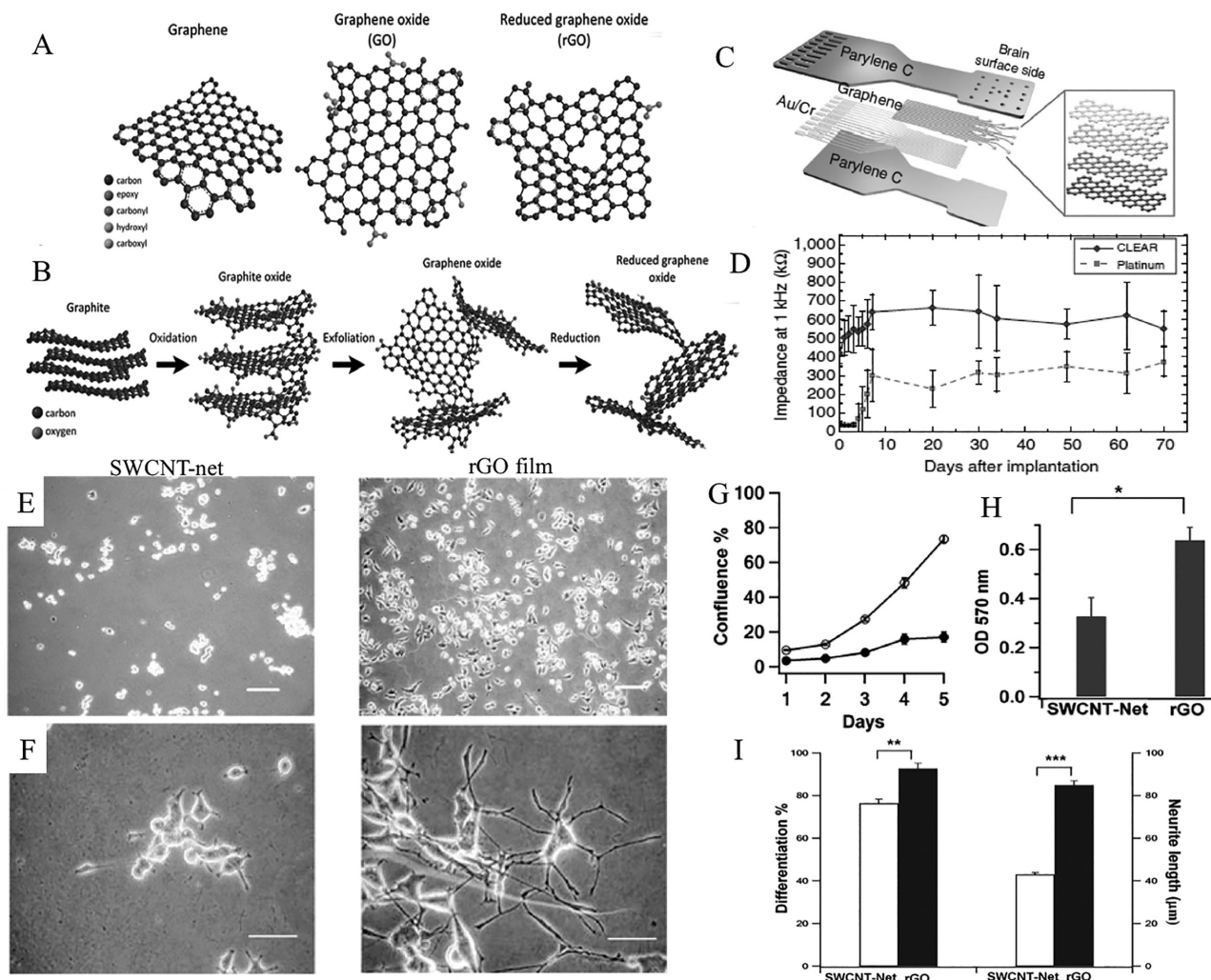


Figure 5. A) Structural differences between graphene, graphene oxide, and reduced graphene oxide. B) Reaction steps of graphite to reduce graphene oxide. Reproduced with permission.^[154] Copyright 2016, InTech. C) Schematic diagram of the CLEAR device. D) In vivo impedance value of CLEAR and platinum micro-ECoG at 1 Hz. Data shown as mean \pm SD of impedance extracted from 16-channel measurement. Reproduced with permission.^[160] Copyright 2014, Nature Publishing Group. E) 5 days of cell culture. Scale bars = 100 μ m and F) neuronal differentiation of PC12 cells on SWCNT-net and rGO film. Scale bars = 50 μ m. G) Confluence percentage of PC12 cells when cultured with SWCNT-net (black circles) and rGO (white circles) for up to 5 days. Data are shown as mean \pm SE. H) Cell viability assay (MTT) showing cell metabolic activities. PC 12 cells were cultured with SWCNT-net or rGO film for 4 days. Data are shown as mean \pm SE, N = 3. I) Left: PC12 cells differentiation percentage. Mean \pm SE are from >1000 cells on three samples and; Right: average neurite length treated with nerve growth factor (100 ng mL⁻¹) for 4 days. Data calculated from 90 cells on three samples. Reproduced with permission.^[163] Copyright 2010, American Chemical Society.

In addition, according to a previous study conducted by Zhou et al., rGO modified glassy carbon (CR-GO/GC) electrodes showed high electrochemical activity with a coefficient of 0.092 cm² (compared to GC electrodes = 0.0706 cm² and graphite/GC = 0.0560 cm²), as calculated from chronocoulometric curves. In AC impedance experiments, CR-GO/GC also exhibited minimum impedance (160.8 Ω) as compared to GC (200.7 Ω) and graphite/GC (407.6 Ω) electrodes.^[156]

However, there are drawbacks associated with the 2D structure of graphene. Due to its flat surface, charge transfer capacity is largely limited and sheet resistance is relatively high^[157,158] Consequently, the intensity and efficiency of electrostimulation will be hindered. To address this problem, various electrocorticography (ECoG)-based arrays have been developed by different

groups to record and stimulate neural signals with minimum invasion and improved signal quality.^[159,160] For instance, Park et al. developed a graphene-based, carbon-layered electrode array (CLEAR) device that can be implanted onto the brain surface to record high-resolution signals (Figure 5C). Apart from conventional ECoG devices that contain either opaque conductive metals that are impossible to stimulate directly at the interface, or transparent indium-tin oxide (ITO) composites that are fragile and only show spectrum-dependent transparency, CLEAR presented broad-spectrum transparency and mechanical flexibility. Briefly, the CLEAR device was fabricated by coating parylene C onto a silicon substrate via chemical vapor deposition (CVD). Traces and pads were then patterned with gold using electron beam evaporation. Four layers of graphene

were subsequently coated onto the parylene surface by wet transfer, and the device was removed from the silicon wafer. In order to leverage the conductivity and the transparency of the material, the sheet resistance and transmittance of different graphene layers was measured. Results indicated that four layers of graphene achieved the best balance with a decrease of 76 Ohms per square in resistance compared to one graphene layer while retaining 90% transmittance.^[160,161] In addition, to assess the overall performance of CLEAR *in vivo*, impedance, baseline signal and electrical-evoked potentials were measured and compared with those of conventional platinum micro-ECoG arrays in rodents (Figure 5D). The CLEAR device presented similar capability with platinum ECoG in impedance control and signal pick-up. Moreover, it exhibited better performance in fluorescence and optical coherence tomography (OCT) imaging owing to broader spectrum transparency.

Another study reported by Lu et al. proposed a porous graphene-coated polyimide electrode fabricated by laser pyrolysis, which can potentially eliminate the delamination phenomenon generated during the coating procedure. This flexible ECeG array succeeded in increasing the charge injection capacity (CIC) of the neural electrode from as low as 0.15 mC cm⁻² in conventional platinum electrodes to 3.1 mC cm⁻² while retaining high flexibility and low impedance.^[162] Results from the *in vivo* study also proved that the device was able to record even weak potentials with a high signal-to-noise ratio.^[159]

4.2.3. Mechanical Properties and Biocompatibility

As one of the thinnest yet strongest materials ever discovered, graphene has an intrinsic tensile strength as high as 120 GPa *in situ* and a stiffness (shown in Young's modulus) of 1.02 ± 0.03 TPa.^[164] In comparison, the stiffness of SWCNT and MWCNT range from 0.27 TPa to 1.47 TPa.^[165,166] Although carbon-based nanomaterials like graphene and CNTs are historically significant in the field of electronics, these materials can potentially be cytotoxic due to their role in generating reactive oxygen species (ROS) *in vivo*.^[167] Therefore, biocompatibility, in addition to mechanical flexibility and tissue compliance, of the implanted electrodes remains a big challenge for graphene-based neural interfaces. To address this, several studies on the biocompatibility of graphene-based materials have been carried out *in vitro* but the results vary. For example, by comparing the mitochondrial activities and membrane integrity of PC 12 cells between graphene and SWCNT using the 3-(4,5-dimethylthiazol-2-yl)-2,5-diphenyltetrazolium bromide (MTT) assay and lactase dehydrogenase (LDH) assay, Zhang et al. demonstrated that graphene had better cytocompatibility at high concentrations (≈100 μg mL⁻¹) over SWCNT but induced more cell apoptosis at low concentrations (≈10 μg mL⁻¹).^[167] On the contrary, Yi et al. concluded that there was no obvious cytotoxicity to PC 12 cells when the graphene concentration was below 20 μg mL⁻¹. However, both studies shared the observation that if the concentration increased from 20 to 100 μg mL⁻¹, ROS levels would significantly increase and toxic effects towards cells would begin to emerge.^[168] More recently, Fabbro et al. conducted a series of experiments with graphene-based substrates (GBSSs), liquid phase exfoliation graphite (LPE-GBS)

and ball milling graphite (BM-GBS), and evaluated their biocompatibility towards brain cells *in vitro*. A comparison of the neural input resistance and cell capacitance values of LPE-GBS and BM-GBS relative to peptide-free control substrates showed that both LPE-GBS and BM-GBS had no negative impact on neuronal cell growth. Biocompatibility was further evaluated by measuring postsynaptic currents (PSCs) with different substrates individually. The intact integrity of the neuronal synaptic network demonstrated that the GBS acted as an inert interface and had no effect on normal tissue behavior.^[169]

Although more data is required to have a clearer understanding concerning the minimum toxic dose of graphene, there seems to be a better agreement on the biocompatibility of rGO. In a study published in 2010, Agarwal et al. introduced reduced graphene oxide (rGO) films and single-walled CNTs network (SWCNT-net) to PC12 neural cells and osteoblasts, and compared both their conductivity and biocompatibility *in vitro* (Figure 5G–I). According to the results, the sheet resistance of the rGO film (3 kΩ sq⁻¹) was significantly lower than that of the SWCNT-net (100 kΩ sq⁻¹). Moreover, cell viability and neurite-growth of PC 12 cells indicated that the rGO outperformed the SWCNT-net in facilitating cell proliferation as well as in inducing more neurite outgrowth. In addition, unlike CNT, graphene produced by chemical or thermal reduction of graphite oxide (GO) did not contain any transition metals (i.e., Fe or Ni) and therefore should enable higher purity for electrocatalytic studies of carbon materials.^[163] A very recent research published by Mendonça et al. further evaluated the *in vivo* toxicity by administering rGO intravenously in rats. In this study, neuron and astrocyte cytotoxicity, nephrotoxicity and hepatotoxicity were assessed. Specifically, motor abnormalities such as dyspnea and convulsions, were evaluated and rats treated with rGO didn't show any neurotoxic symptoms.^[170] In addition, neurotoxicity in tissues, such as the hippocampus, was investigated. Histological stains of the hippocampus were conducted to evaluate inflammation and necrosis. Neuronal viability was also evaluated by measuring nuclear antigen protein (NeuN) levels. Results indicated that neurotoxicity slightly increased at 15 min post-administration but returned to normal level at 1, 3 h and 7 days post-administration. As a conclusion, although a limited short-term toxic effect was recorded after administration, rGO didn't induce any significant neurotoxicity nor alter neuron morphology 7 days post administration.^[171]

In summary, the exceptional electrical and mechanical properties of graphene and graphene derivatives have been studied by various groups, and promising *in vitro* results presented. Admittedly, graphene-based materials have attracted widespread attention due to their potential applications in neural electrodes, biosensors, and drug delivery systems. However, information quantifying their long-term toxicity and stability *in vivo* require further input and investigation.^[144]

4.3. Carbon Nanotubes (CNTs)

4.3.1. Overview of Carbon Nanotubes (CNTs)

Carbon nanotubes (CNTs) are hollow cylinders formed by one (single-walled CNTs, SWCNTs) or several (multi-walled CNTs,

MWCNTs) layers of graphene (Figure 6A–C).^[172] As mentioned above, CNTs can be fabricated via a variety of methods, including chemical vapor deposition (CVD) and arc-discharge, and they have garnered high interest in a number of different fields due to their unique mechanical, chemical, and electrical properties.

4.3.2. Mechanical and Electrical Properties

The electronic properties of CNTs depend on their geometric construction. SWCNTs can exhibit either semiconducting or metallic conductivity depending on their chirality (i.e., the angle at which the graphene sheet is rolled),^[173] whereas MWCNTs show only metallic behavior.^[174,175] While early synthesis

procedures were only capable of producing mixtures of metallic and semiconducting SWCNTs, Chen and colleagues designed a process to simultaneously assemble and separate the two classes of SWCNTs via a dielectrophoretic mechanism.^[176] In all of their forms, CNTs exhibit a wide electrochemical window,^[177] and the magnitude of currents that can be achieved, typically scale with the area of exposed CNTs.^[178]

In combination with their high conductivity, the dimensions of CNTs make them well-suited for applications within neural electrodes. CNTs morphologies resemble neurites^[179] and their structural features share similarities with those of the neural machinery (ion channels, signaling proteins, elements of the neuronal cytoskeleton, and others).^[180] In general, smaller electrode sizes are desired in order to gain improved spatial resolution of electrical signals within neural

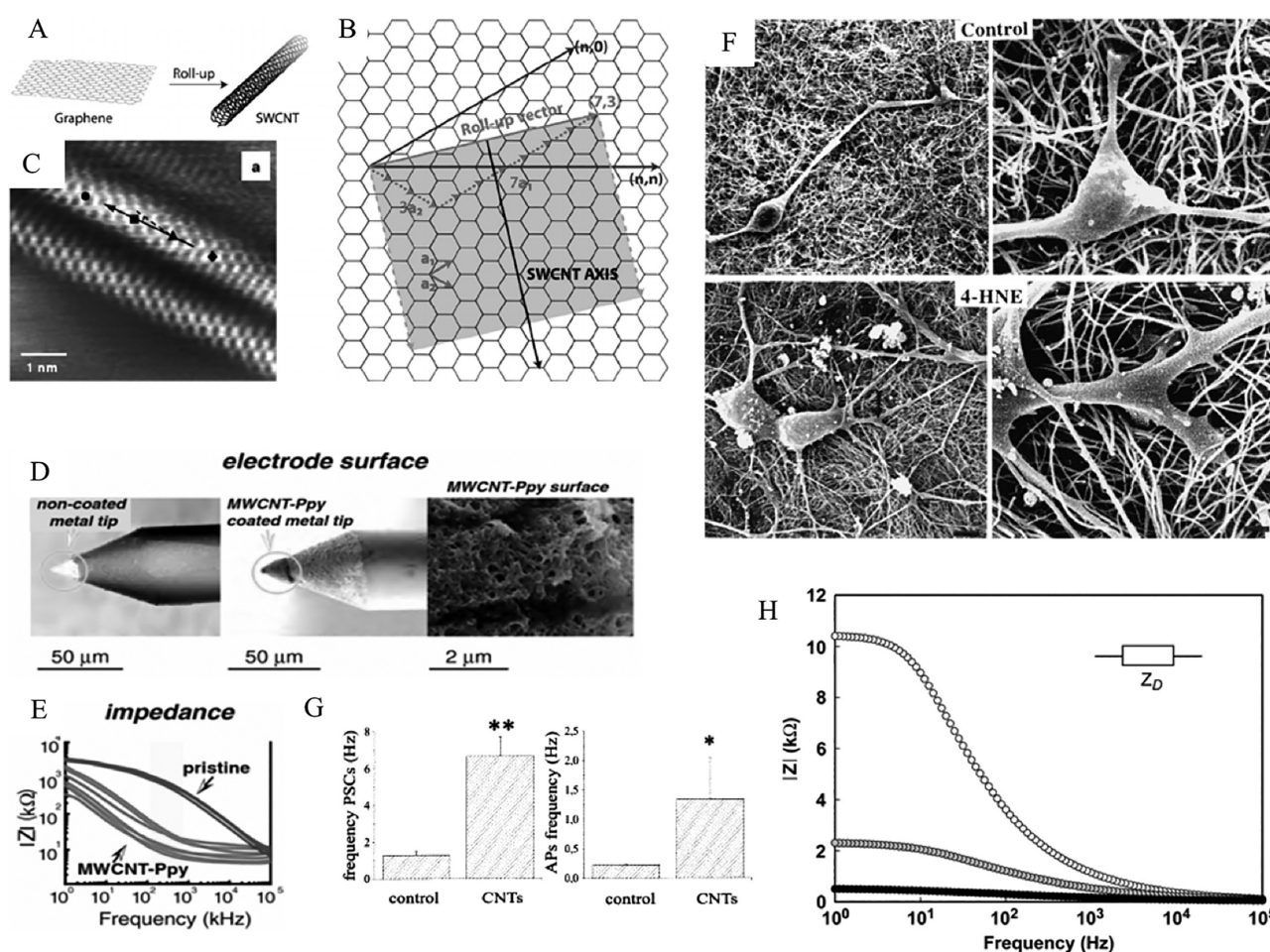


Figure 6. A) Single-walled carbon nanotubes (SWCNTs) can be created by rolling up a monolayer of graphene.^[210] B) Rolling the graphene sheet along different vectors results in CNTs with different structures.^[210] C) Scanning tunneling microscopy image of a semiconducting SWCNT.^[210] Reproduced with permission.^[210] Copyright 2013, Elsevier. D) SEM images show an uncoated electrode tip (left), a tip coated with MWCNT-PPy (middle), and a high magnification image of the MWCNT-PPy coated tip (right).^[211] E) Impedance spectroscopy showed a significant decrease in the impedance modulus. Reproduced with permission.^[211] Copyright 2011, IOP Publishing. F) SEM images showing neurons grown for 3 d on unmodified control nanotubes (upper) and nanotubes coated with 4-hydroxynonenal (lower). The right panels show portions of the left panels at higher magnification. Scale bars: left panels, 5 μm ; right panels, 100 nm.^[212] Reproduced with permission.^[212] Copyright 2000, Springer. G) Hippocampal neurons grown on CNT substrates exhibited significantly increased spontaneous postsynaptic currents (PSCs) and action potentials (APs). $**P < 0.0001$ and $*P < 0.05$.^[194] Reproduced with permission.^[194] Copyright 2005, American Chemical Society. H) The frequency dependent diffusion impedance (Z_D) of electrodeposited PPY/Cl (top curve), PPY, PPS (middle curve), and PPY/SWCNT (bottom curve) are plotted against frequency.^[213] Reproduced with permission.^[213] Copyright 2010, Elsevier.

tissue. However, one of the major drawbacks to conventional metal electrodes is the increase in impedance that accompanies a decrease in size.^[103,175] This increase in impedance makes the detection of small extracellular potentials very difficult. To overcome this, commonly used electrodes have been modified with CNTs to increase the tip surface area, thus decreasing the microelectrode impedance without significantly affecting the geometrical tip size (Figure 6D,E).^[96] For instance, Keefer et al. coated conventional tungsten and stainless steel electrodes with CNTs.^[181] The CNTs coating enhanced both recording and electrical stimulation of neurons in culture, rats, and monkeys by decreasing the electrode impedance and increasing charge transfer. Chen et al. demonstrated that carbon fiber nanoelectrodes modified with SWCNTs were capable of detecting electrically active analytes from single cells.^[182]

To stimulate a neural response, a minimum charge magnitude must be delivered. However, to avoid irreversible chemical reactions, this value should not exceed the maximum charge injection density of the electrode material.^[103] Additionally, it is important to avoid faradic reactions at the electrode interface that may result in damage to the surrounding tissues.^[183,184] For example, activated iridium oxide provides a high charge injection limit via a reversible faradic reaction,^[185] but it has been reported to delaminate under high current pulses to deposit particles in the surrounding tissue.^[186] In contrast, CNTs deliver current primarily through charging and discharging their interfacial double layer, instead of through faradic reactions.^[104] Thus, via this capacitive mechanism, no chemical change occurs to either the tissue or the electrode during stimulation of neural tissue. Additionally, the maximum charge density for CNT-coated electrodes has been reported to be twice that of similarly sized iridium oxide electrodes.^[187]

4.3.3. Biocompatibility

For interfacing with biological tissues, CNTs can be easily functionalized to improve their solubility in a variety of solvents and to reduce their cytotoxicity.^[188–191] While CNTs undoubtedly possess excellent mechanical and electrical properties, their application for neural interfaces requires that they should not elicit negative biological reactions that could dampen electronic communication (i.e., resulting from inflammation or glial scar formation) or more importantly, damage neurons. Unmodified (pristine) CNTs are often considered non-biocompatible, or toxic towards biological tissues.^[180,192,193] However, CNTs can be easily modified to improve their biocompatibility. For example, Mattson et al. reported that neurons grown on unmodified CNTs did not spread out appreciably, whereas neurons grown on CNTs coated with the bioactive molecule 4-hydroxynonenal extended multiple neurites with extensive branching (Figure 6F).^[192] After unsuccessful attempts at preparing a substrate of unmodified CNTs, Lovat et al. functionalized the CNTs with pyrrolidine to increase their solubility in organic solvents, which allowed a lawn of CNTs to be coated onto glass. The organics and functional groups were subsequently heated away, and single-cell patch-clamp recordings indicated that

hippocampal neurons grown on CNTs exhibited significantly higher electrical network activity compared to neurons grown on glass control substrates (Figure 6G).^[194]

Functionalization of CNTs can be accomplished by either covalent or non-covalent interactions.^[180] Non-covalent functionalization allows the preservation of the aromatic structure of CNTs without damaging their electronic characteristics,^[180] and can be achieved by combining the CNTs with surfactants, polymers, peptides, or single-stranded DNA.^[195–198] It has been suggested that SWCNTs offer more precise functionalization strategies compared to MWCNTs.^[199,200] Using a streptavidin/biotin system, Shim et al. demonstrated that high specificity can be achieved via SWCNT functionalization.^[201] SWCNTs functionalized by co-adsorption of a surfactant and poly(ethylene glycol) were capable of resisting nonspecific adsorption of streptavidin, whereas SWCNTs co-functionalized with biotin and protein-resistant polymers encouraged the specific binding of streptavidin onto the SWCNTs.

CNTs can be utilized for neural electrodes in a variety of ways, either as part of a composite electrode or by using an individual CNT as the electrode tip. Chen et al. fabricated nanoelectrodes from single CNTs that were connected to tungsten or carbon fiber probes and coated them with an insulating material except at the CNTs apex.^[202] They reported similar electrochemical behavior to the commonly used carbon fiber probes, but noted that the significantly reduced electrode area provided much higher spatial resolution and signal-to-noise ratio. Heller et al. fabricated a similar assembly and demonstrated that the unique geometry of the SWCNT nanoelectrodes allowed them to resolve the kinetics of super-fast electrode reactions.^[203]

Alternatively, several research groups have implemented CNTs within composite electrode designs to achieve desired macro-scale shapes or functions while taking advantage of the geometric and electronic properties of CNTs. He and colleagues noted that SWCNTs provided conductive properties and mechanical reinforcement to soft, non-conductive hydrogels (PEGDA).^[106] Moreover, by encapsulating the SWCNTs within the hydrogel, the cytotoxicity of CNTs was not a concern. Lu et al. electrochemically co-deposited polypyrrole/SWCNT (PPy/SWCNT) films that exhibited a high safe charge injection limit and low electrode impedance at 1 kHz (Figure 6H).^[204] When implanted into the cortex of rats, the electrodes induced significantly lower glial fibrillary acidic protein (GFAP) and higher neuron density in the proximity of the implant. CNTs are highly conductive and can be easily implemented for neural electrodes in a variety of ways, including within microelectrode arrays (MEAs),^[205] or as vertically aligned carbon nanofibers (VACNFs) that assemble into conical shapes to easily interface with cells.^[206] CNTs have been used for electrochemical applications requiring ultra-low detection limits,^[207] and have shown promise in vivo for both neural recording^[107] and stimulation.^[208] For chronic applications, CNTs have even shown promise for directing stem cell differentiation towards the neuronal lineage.^[209] Ultimately, the electronic properties and physical dimensions of CNTs could have a significant impact on the future of neural interfaces.

4.4. Conducting Polymers (CPs)

4.4.1. Overview of CPs

CPs are a class of unique polymers that present alternating single and double bonds along the backbone, a conjugated system that confers semiconductive properties to the polymer by allowing charge mobility along the polymer backbone and between adjacent chains^[214] (Figure 7A). When neutralized and stabilized with appropriately charged dopants via chemical or electrochemical oxidation or reduction during fabrication, CPs can possess metal-like high conductivity.^[113] As an electrical potential is applied, the dopants will act as the charge carriers and move in and out of the polymer, creating

a continuous pathway that allows charge to pass through.^[215] CPs are gaining significant attention for the development of neural interfaces due to their capacities to leverage electrical, mechanical and biological properties. In general, most CPs present a number of unique advantages in the context of neural interfacing, including high charge storage capacity (CSC), low impedance and high injection limit compared to bare metal electrodes.^[24,216] In addition, they have the ability to alleviate the mechanical mismatch between electrodes and neural tissues and to entrap and controllably release biological molecules that help enhance biocompatibility and improve tissue integration (i.e., reduced inflammation and enhanced neuron regeneration). Thus, modification of a neural electrode with CPs has long been suggested to be a promising approach

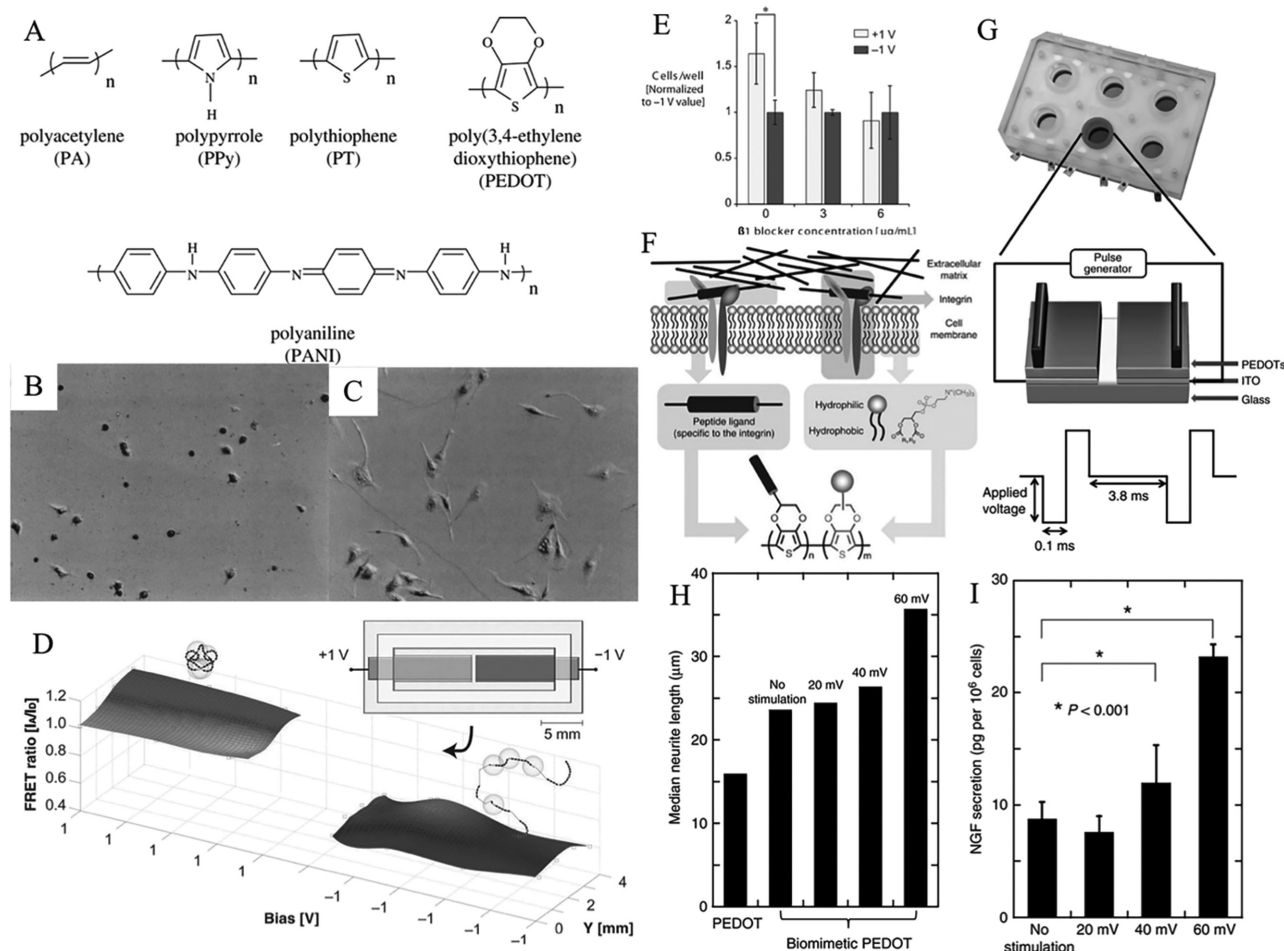


Figure 7. A) Chemical structures of various CPs. Reproduced with permission.^[251] Copyright 2007, Elsevier; B) Endothelial cells cultured for 4 h on FN-PPy in either its native oxidized state, or C) after reduction by the application of -0.5 V for 4 h, indicating that electrical controls can be achieved by switching the redox state of CPs ($\times 700$). Reproduced with permission.^[232] Copyright 1994, National Academy of Sciences; D) FRET ratios on the pixel device as a function of applied bias and position, color of the surface indicates local FN conformation and the corresponding schematics of conformation are shown above the surface. The inset shows the device configuration; E) Relative number of adherent 3T3-L1 mouse fibroblasts on fully oxidized (+1 V) and reduced (-1 V) pixels, for varying doses of a $\beta 1$ function-blocking antibody. Reproduced with permission.^[238] Copyright 2012, Wiley; F) Schematic representation of the approach leading to the design of the target conductive polymer, mimicking the interactions between a cell membrane and the ECM; G) Schematic representation of the device used for cell growth with applied electrical stimulation; H) Median neurite length of PC12 cells on PEDOT and biomimetic PEDOT in the absence and presence of an applied pulsed electrical stimulation at amplitudes of 20, 40 and 60 mV; I) NGF secretion from primary Schwann cells cultured on biomimetic PEDOTs (prepared from 3 mm EDOT-MI and 7 mm EDOT-PC, conjugation with RGD) in the absence and presence of an applied pulsed electrical stimulation at amplitudes of 20, 40 and 60 mV. Reproduced with permission.^[243] Copyright 2014, Nature Publishing Group.

in developing stable long-term neural implants with improved performance.

4.4.2. Electrical Properties

One of the important reasons that CPs can be used to establish a stable and effective communication link between biotic and abiotic systems are their excellent electrical properties, like high charge storage capacity (CSC), high injection limit and low impedance.^[214] One of the benefits of CP coatings lies in lowering the electrode impedance, and hence a decrease in the voltage needed to achieve a stimulation effect similar to that of a conventional metal electrode. This can potentially reduce harmful electrochemical side reactions. In neural recording applications, a decrease in impedance can lead to better recording with a high signal-to-noise ratio (SNR).^[196] Cui et al. reported that CP coatings can significantly reduce the impedance of metal electrodes by up to two orders of magnitude at 1 kHz.^[122] CSC improvement is another advantage of applying CP coatings. Green and co-workers demonstrated that PEDOT-coated Pt electrodes possessed a CSC of up to 130 mC cm⁻², whereas Pt alone has values of around 6 mC cm⁻².^[24] Simultaneously, it was discovered that the charge injection limit of PEDOT was 30 times larger on average than that of Pt, which is beneficial for applications in which a high voltage is required.

Although CP coatings have the potential to provide enhanced electrical performance, there is the prevailing concern that factors like repeating cycling cause a loss in electroactivity over time. One of the examples can be found in the case of a PPy/PSS film, in which a 95% loss in conductivity was observed after 16 hours of polarization at 400 mV.^[217] This was largely attributed to the loss of dopant molecules that occurred during stimulation. Several strategies for improving electrochemical stability have been proposed, including layering of a polymer^[218] with complementary properties and more commonly, the incorporation of CNTs.^[83,204,219] Results thus far demonstrate that improved stability, enhanced cell adhesion and neurite outgrowth, and lower tissue responses are possible.

4.4.3. Mechanical Properties

Traditional electrodes fabricated with pure metallic materials are mechanically hard with a modulus of 50–500 GPa, and in their conventional form, they are fairly inelastic and have limited flexibility in 3D.^[220] A mismatch in mechanical properties and structural rigidity can lead to shear, which results in chronic inflammation of the surrounding tissue and ultimately isolation of the electrode.^[214] Isolation of the electrode leads to a reduction in effective signal transfer, which is purported to cause a decrease in electrode performance. Developing alternative, soft materials with biomimetic mechanical properties is therefore of key importance to overcoming these challenges. Since CPs generally have a low modulus of around 1 MPa to 5 GPa, using CP coatings has been explored as a strategy for improving the mechanical properties of the electrodes and

providing a conformable and adaptable interface.^[138,220] Sparse data produced from microtensile tests showed that a PPy/pTS film can have a Young's Modulus from anywhere between 1.2 to 3.6 GPa, depending on the electrolyte used as well as the voltage applied.^[221] More recent studies further demonstrated that the modulus of PEDOT-based CP films falls in the range of 1–3 GPa,^[222,223] however, when hydrated, the Young's modulus of PEDOT/PSS can be as low as 40 MPa. Admittedly, although this is at least three orders of magnitude higher than that of neural tissues (≈ 1 kPa),^[224] it still represents a substantial leap from the metallic electrode. Additionally, since the conductivity of CPs is not as high as one would want it to be, they must be patterned on more rigid substrates, such as metals and silicon, which still dominate the overall stiffness of the electrode shank. The conductive polymer coatings, however, do dampen or mediate the mechanical differences/mismatch at the immediate interface between the electrode and the tissue. It is also worth noting that mechanical properties of the material in contact with the cells also have tremendous effects on their biological behavior as evidence has shown that cells can sense local matrix stiffness, which in turn are likely to have important implications for the cell development and differentiation.^[225] In this sense, although the same issue of mechanical mismatch is still present, the addition of a conductive polymer coating does provide an opportunity in mediating interfacial mechanical mismatch and modulating cell behaviors. Additionally, the problem of mechanical mismatch can be further alleviated by the incorporation of a hydrogel as described in section 4.5.

Although evidence suggests the potential of CPs to reduce mechanical mismatch, many studies so far have been limited to in vitro and sub-chronic in vivo assessment. In an experiment carried out by Ouyang et al., PEDOT polymerized in vivo in a living rat hippocampus showed an optimal decrease in impedance within 3–4 weeks without causing significant deficits in performance of a delayed alternation task.^[226] However, more in vivo evidence under chronic implant conditions has to be presented to fully characterize the benefit of applying CPs to a neural electrode.^[227] Even if CP films may theoretically be able to alleviate the mechanical mismatch at the electrode-neural interface, mechanical stability remains a great concern for chronic applications. One such concern that stands in the way is the delamination of CP coatings in vivo, which can be further accelerated by repeated volume changes at the interface driven by the expulsion of dopants or incorporation of ions from the electrolyte^[215] during electrical stimulation. In response to the high interest in developing stable CP coatings for chronic applications, several improvement strategies have been proposed. For example, laser roughening of the underlying metal substrate has been shown to significantly improve adhesion of PEDOT based systems without affecting the charge injection limit of the coated material.^[228] Other techniques to increase the bonding strength between metal substrate and CPs include the use of a “fuzzy gold” layer as an adhesion promoter for PPy coatings,^[229] the adoption of chemisorbed EDOT-acid as an adhesion enhancer between PEDOT and indium thin oxide (ITO),^[230] and the inclusion of dopamine as a bio-inspired adhesive molecule during electrochemical polymerization of PPy onto ITO.^[231]

4.4.4. Biocompatibility

Although the immediate interface has been electronically and mechanically improved in recent years, continued development is pivotal in translating current CP coating technologies into the clinic. However, there is a need to develop long-term implants that circumvent a foreign body response and integrate well with surrounding tissue. Towards this end, a lot of effort has been given to investigate CP-cell interactions. The first ever use of a CP inside a biological environment was led by Langer and co-workers. Inspired by the reversible charge density and wettability through electrical stimulation, they were able to illustrate that reducing fibronectin-coated-PPy to its neutral state by electrical stimulation inhibited aortic endothelial cell spreading and DNA synthesis (Figure 7B,C).^[232] The same group later applied similar principles on neuronal cells (PC-12 cells) and demonstrated that cells electrically stimulated by a PPy substrate resulted in almost a two-fold increase in neurite outgrowth.^[233] Subsequent studies indicated that the enhanced neurite extension might be due to the increase in adsorption of serum proteins, especially fibronectin, upon electrical stimulation.^[234] They further proved that electrical stimulation is only effective when immediately applied, while in delayed stimulation, in which fibronectin was allowed to adsorb for 2 h, no significant difference was observed between stimulated and unstimulated groups. This was possibly due to high protein adsorption within the first 2 hours of exposure. However, more recent experiments indicated that protein adsorption might not be the only factor responsible for cell adhesion and growth. In a study done by Saltó et al., better adhesion and proliferation of neural stem cells were found on the oxidized side, while interestingly, stronger and denser protein binding were found on the reduced side.^[235] Similar results were obtained during an effort to electrically control cell density along a redox gradient of PEDOT.^[236] Maximum cell adhesion was achieved at either extreme but rather somewhere in between. Similar principles have been applied to control epithelial cell-density gradients along an electrochemical transistor;^[237] however, the underlying mechanism still remains elusive. It was not until 2012 that Wan and co-workers ascertained the importance of fibronectin conformational changes on cell adhesion during electrical stimulation of CPs. Significantly higher cell adhesion was found on the oxidized site where fibronectin compactly folded (Figure 7D,E).^[238] Only by understanding these underlying mechanisms can we rationally design proper CP coatings that promote tissue electrode integration.

In addition to being electronically active, CP coatings, unlike conventional metallic or inorganic semiconductor electrodes, can be appended by functional molecules, such as extracellular matrix (ECM) molecules or anti-inflammatory molecules. These can be easily incorporated via simple adsorption, entrapment, covalent binding or doping^[215] to encourage neural attachment and to reduce the likelihood of an inflammatory response. One of the most heavily investigated molecules to improve the biological responses of CP coatings is ECM or ECM protein derived molecules due to their well-known role in regulating cell attachment, proliferation, differentiation, migration and apoptosis.^[239] It has been demonstrated that scaffolds containing small, degradable polymer beads that release nerve

growth factors (NGF) to mimic the chemical microenvironment of developing tissue, improve the viability of fetal neural cells transplanted into rat brains.^[240] Incorporation of ECM molecules and mediating their activated release has been one of the leading strategies for improving the biological responses of CP coatings. For example, oligopeptides like RGD^[241,242] and YIGSR^[128] have been introduced into PPy and PEDOT coatings, leading to increased cell adhesion in vitro, stronger connections with the neuronal structure, and improved recordings at coated sites. A recent study carried out by Zhu et al.^[243] developed a cell membrane-mimicking CP with oligopeptide modification and was shown to resist nonspecific cell binding and recognize neural cells specifically to allow intimate electrical communication (Figure 7F,G). Both enhanced neurite outgrowth and increased secretion of proteins from primary Schwann cells under electrical stimulation were also demonstrated (Figure 7H,I). Similarly, fibrillar collagen,^[244] nerve growth factors,^[245,246] and neurotrophic proteins^[247] have been immobilized into CP coatings and have been shown to promote cell survival, attachment, extension and differentiation. However, concerns over foreign body responses limit their application in chronic neural interfaces. In one study, although improvements in neural attachment and neural recordings were observed at an early stage, fibrotic tissue formation ultimately isolated the electrodes from the target tissue, rendering the electrode ineffective.^[128] Toward this end, anti-inflammatory molecules have been proposed for mitigating the initial inflammatory reaction as well as the ongoing presence of fibrotic reactions at the neural interface.^[248] The switchable redox state of the CPs theoretically provides a unique opportunity to create stimuli responsive drug delivery systems that can release drug molecules on-demand through electroactivation. As a proof of concept, an anti-inflammatory drug, dexamethasone, has been successfully incorporated into PEDOT nanotubes^[115] and PPy films,^[249,250] and the release of the drug can be precisely controlled through external stimulation with minimal toxicity to neuronal cells. CP-coated electrodes hold significant benefits over the conventional metallic electrodes by addressing some of the limitations associated with mechanical mismatch and foreign body response and providing superior electrical, mechanical and biological properties. However, designing an optimized scaffold for neural interfacing requires a tradeoff between these properties. Furthermore, despite the enhanced performance of CP coated electrodes, concerns remain for mechanical stability and chronic inflammation reactions. More in vivo evidence still needs to be presented in the future to fully assess their benefits under chronic implant conditions.

4.5. Hybrid Nanomaterials

While the electroactive materials discussed above individually offer some aspects of chemical, mechanical, or biological stability compared to conventional metallic electrodes, none possess a complete set of properties necessary to maintain optimal performance at neural interfaces for long periods of time in vivo. For example, although CPs provide enhanced electrical properties and alleviate some of the limitations associated with mechanical mismatch between electrodes and brain tissues,

inadequate mechanical stability (i.e., delamination under mechanical stresses and wet conditions) as well as fibrous capsule formation remain that prevent them from maintaining optimal performance in biological environments. Recall that CNTs possess remarkable electrical properties, however, CNTs are extremely stiff materials with a Young's modulus in the range of TPa,^[252] and the significant mechanical mismatch can lead to chronic inflammation at neural interfaces. Furthermore, CNTs do not simply adhere to the electrode surface. They require additional processing, such as chemical modification or incorporation within a polymer matrix.^[214] It is also worth noting that the biocompatibility of CNTs is still a subject

of large debate, the results of which depend mostly on their purity.^[253]

Efforts have been devoted towards developing composite scaffolds that combine complementary properties of electroactive materials (i.e., CPs, CNTs or graphene).^[146,204,254–257] Although enhanced electroactivity, mechanical stability, and biocompatibility have been illustrated, not enough evidence has been obtained to demonstrate the benefits of these materials in a chronic implant environment. Mechanical mismatch as well as the resulting inflammation due to micromotion are also a challenge.^[214] For example, co-deposition of PPy and SWCNT onto Pt microelectrodes (Figure 8A) was shown to increase the

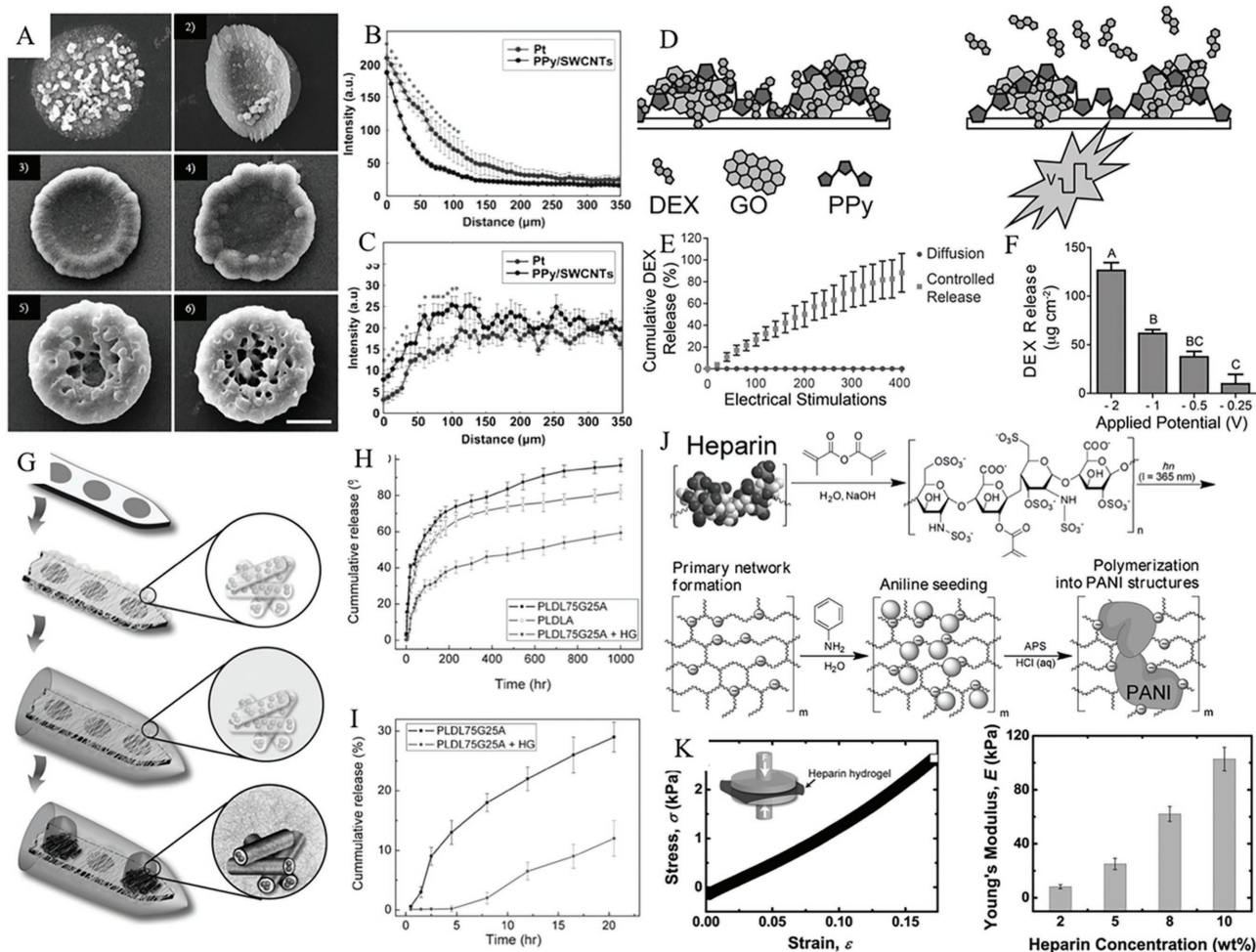


Figure 8. A) SEM images of electrodeposited PPy/Cl (1), PPy/PSS (3) and PPy/SWCNT (5) film electrodes under optimal conditions and morphological changes after electrical stimulation (2, 4, 6) (scale bar is 50 μm); B) A quantitative comparison between the control and deposited implants was made via GFAP intensity profiles as a function of distance from the implant interface; C) Quantitative evaluation of the survival of neurons around the implanted site using NeuN staining. Reproduced with permission.^[204] Copyright 2010, Elsevier; D) Drug loading into and release from the GO/PPy nanocomposite in response to electrical stimulation; E) Cumulative release profile of the GO/PPy-DEX nanocomposite in response to milder release stimulation (-0.5 V for 5 s, followed by 0.5 V for 5 s) and in the absence of electrical stimulation (passive diffusion); F) Effect of voltage stimulus modulation on amount of DEX released from nanocomposite films. Bars labeled with nonmatching letters indicate a significant difference between groups ($p < 0.01$, $n = 3$). Reproduced with permission.^[261] Copyright 2014, American Chemical Society; G) Schematic diagram of the fabrication process for multifunctional polymer coatings on the neural microelectrodes, PEDOT was electrochemically polymerized around the DEX-loaded electrospun biodegradable nanofibers within the hydrogel scaffold; H) Percentage cumulative mass release profiles of DEX-loaded PLDLA nanofibers, PLDL74G25A nanofibers, and alginate hydrogel-coated PLDL74G25A nanofibers, over 1000 h, and (I) a zoom window of (H) for PLDL74G25A nanofibers, and alginate hydrogel-coated PLDL74G25A nanofibers, over the first 20 h. Reproduced with permission.^[127] Copyright 2009, Wiley; J) Synthetic scheme of biologically derived soft conducting hydrogels using heparin-doped polymer networks and K) the corresponding Young's modulus at varying heparin concentrations. Reproduced with permission.^[287] Copyright 2014, American Chemical Society.

safe charge injection limit dramatically to $\approx 7.5 \text{ mC cm}^{-2}$, to decrease impedance at 1 kHz (reduced by 95%), and to improve mechanical and electrochemical stabilities as compared to pure CP films. Histological analysis revealed a decreased expression of glial fibrillary acid protein (GFAP), which is a specific marker of astrocytes, as well as higher neuronal density in the vicinity of the implant (within $\approx 100 \mu\text{m}$) (Figure 8B,C).^[204] More recently, graphene-based composite materials in combination with either CPs or CNTs were also explored to take advantage of their exceptional electrical and physical properties, such as high electrical conductivity^[258] and great mechanical strength.^[145] In one case, sulfonated graphene (SG) sheets were used as conductive dopants for the CP PPy, and the introduction of SG sheets into the nanocomposite film improved both conductivity and electrochemical stability compared to PPy films. Results showed that they exhibited a mass specific capacitance as high as 285 F g^{-1} at a discharge rate of 0.5 A g^{-1} and maintained 92% of capacitance after 800 charging/discharging cycles.^[254] Similarly, in another study carried out by Parker et al., graphitic foliates were grown along the length of aligned MWCNTs, which resulted in over a 500% increase in weight specific capacitance.^[255] With advancements in the ability to bio-functionalize graphene-based materials with biomolecules, such as DNA, proteins and peptides, these materials have started to receive enormous attention in biomedical applications.^[259]

One such area is to use functional graphene-based nanocomposites as a substrate to interface with cells. As exemplified in a study by Luo et al.,^[260] partially embedded graphene oxide (GO) sheets in a GO/PEDOT nanocomposite were bioconjugated to a laminin derived p20 peptide, which was designed to promote neurite outgrowth. Results confirmed that the nanocomposites were indeed able to permit the enhanced growth of rat primary neurons while possessing low impedance and good biocompatibility characteristics necessary for neural interfacing. In another study, GO/PPy nanocomposites demonstrated their advantages over a control PPy film in its higher drug loading capacity (over a two-fold increase) and its highly controllable and tunable drug release profile^[261] (Figure 8D). By incorporating an anti-inflammatory drug (dexamethasone) and electrically controlling its subsequent release (Figure 8E,F), it was demonstrated that these materials could interrupt astrocyte proliferation while having minimal toxicity on neurons. In spite of the superior electrical, mechanical, and biological properties of these composite materials, none of them fully address the issues with chronic inflammation partly due to mechanical mismatch between implanted materials and native tissues, which accounts for implant inconsistency or failure in the long term. Additionally, the toxicological profiles of both CNTs and graphene-based nanomaterials are still far from being fully elucidated.^[262,263]

In this sense, there is an urgent need for more biocompatible materials that can bring together the advantageous electrical properties of individual materials while minimizing mechanical mismatch and instability. Besides, recent evidence suggests that neuronal viability, although necessary, might not be sufficient for favorable performance in chronic applications. Persistent inflammation at the implantation site can lead to a neurodegenerative state,^[264] which can disrupt the normal network connectivity between the electrode and neuronal cells

required for satisfactory sensitivity. Consequently, researchers are seeking softer interfacing materials that encourage and guide neuronal survival, migration, and growth. One such promising material that is actively being pursued for improving neural interfacing is the hydrogel. Hydrogels are three-dimensional cross-linked networks of hydrophilic polymers derived from natural or synthetic sources^[265] that are similar to biological tissues and can have extremely high water content of up to 99.7%.^[266] They have been extensively investigated for the purpose of tissue engineering and smart drug delivery systems due to their highly tunable biological and physical attributes^[267] and their excellent diffusion, or sustained release, of incorporated molecules.^[265] In the area of neural tissue engineering, hydrogels have been considered as one of the most promising platforms since they can be rationally designed to: 1) have the proper modulus to promote cell survival^[268] and optimize neurite branching and extension;^[269] 2) adopt the preferable architecture, such as overall shape and pore sizes, to allow for cell growth and extension;^[270,271] and 3) possess favorable degradation kinetics that contribute to the temporally controlled release of incorporated molecules and to the prevention of immune responses often associated with implanted devices.^[272]

Due to above stated reasons, hydrogels as coating materials have gained considerable interest for improving long-term performance of neural electrodes. In a design by Lu et al., poly(vinyl alcohol)/poly(acrylic acid) hydrogel (PVA/PAA hydrogel) coatings were developed due their excellent biocompatibility, tunable mechanical properties, and good film forming properties.^[273] It was reported that PC12 cells were more cytocompatible on such coated surfaces, achieving much higher densities and promoting neurite extensions. Immunohistological assays 6 weeks after implantation found that GFAP levels were significantly lower in coated groups near the electrode surface ($\approx 150 \mu\text{m}$). In a follow-up study by the same group, a polyethylene glycol (PEG) containing a polyurethane (PU) hydrogel was also identified as a favorable electrode coating material.^[274] It was demonstrated that the PEG/PU coating was able to attenuate glial scarring and reduce neuronal cell loss around implants. This was hypothesized to result from a reduction in protein absorption ($\approx 93\%$) on the electrodes. The idea of incorporating neurotrophin^[275] or an anti-inflammatory agent^[276] into hydrogel coatings was also actively pursued and was shown to hold promise in bringing neurons closer to the surface as well as in reducing the inflammation and the formation of the low-conductive gliotic layers, which contributed to maintaining in vivo impedance of implanted electrodes for over 2 weeks. Although results showed the minimization of a tissue response and the generation of neurite extensions, pure hydrogel coatings can suffer from a loss of electrical properties in many cases due to the inability of polymers to conduct electrons efficiently.^[277] For example, impedance of the microelectrodes increased from $3.3 \text{ k}\Omega$ to $5.5 \text{ k}\Omega$ and $6.3 \text{ k}\Omega$ for PVA/PAA and PEG/PU coatings, respectively. CSC also decreased slightly from 55 mC cm^{-2} to $\approx 48 \text{ mC cm}^{-2}$ in the case of the PVA/PAA hydrogel. Fortunately, recent research suggests that the decrease in electrical performance could be reverted by blending hydrogels with electroactive materials, such as CPs,^[127,278–284] CNTs,^[106,285] and graphene.^[286]

One of the first attempts to incorporate CPs into hydrogel scaffolds was conducted by Kim and his colleagues.^[281] PPy/PPS was successfully vertically grown through the alginate hydrogel deposited on the surface of the microfabricated neural prosthetic probes. The addition of PPy was shown to reduce the impedance of the coating drastically by more than two orders of magnitude to around 7 k Ω at 1 kHz and to increase the charge storage density significantly to 560 $\mu\text{C cm}^{-2}$ (compared to 6 mC cm^{-2} for platinum and 61 mC cm^{-2} for activated iridium). Although no direct evidence on biocompatibility was presented, it was hypothesized that the presence of a hydrogel layer would presumably allow the incorporation of growth factors or anti-inflammatory drugs with little or no change in impedance. The reduction in impedance would promote more efficient signal transport with neurons. Since then, combining CPs with hydrogels has become one of the mostly widely investigated strategies in developing robust and reliable chronic neural implants. In the following study, another CP, PEDOT, was also successfully incorporated into an alginate hydrogel and evaluated for its role in improving the recording functionality of the hydrogel-coated electrodes.^[280] It was demonstrated that these CP/hydrogel coatings were able to improve SNR of coated electrodes significantly from 3.91 to 4.17, indicating their potential to facilitate more efficient signal transmission.

To fully realize the potential of hydrogel-based nanocomposite in reducing inflammation and encouraging neuronal growth, anti-inflammatory drugs^[127] or biologically relevant molecules, such as arginine-glycine-aspartic acid (RGD) peptides,^[282] have been incorporated. Abidian et al. proposed a 3D alginate hydrogel scaffold that contains dexamethasone encapsulated PLGA fibers deposited with PEDOT^[127] (Figure 8G). The alginate coating was shown to not only slow down the release of dexamethasone in a period of 5 weeks but also reduce the burst release effect by about 40% without compromising its superior electrical properties (Figure 8H,I). To improve the function of cochlear implants, Chikar and co-workers proposed the integration of a brain-derived neurotrophic factor (BDNF), RGD-functionalized alginate hydrogel, and PEDOT, with the hypothesis that RGD-functionalized hydrogels can act as artificial ECMs that support neuronal and tissue growth.^[282] It was reported that the PEDOT coating reduced electrode impedance at all frequencies measured *in vitro*. The reductions in impedance were a function of coating thickness. When incorporated into a hydrogel via direct soaking, BDNF was released from the hydrogel into the cochlear at a biologically significant level, 28.13 ng mL^{-1} , 1 week post-implantation, and 13.91 ng mL^{-1} at 2 weeks post-implantation. This indicated its potential to modulate biological behavior via growth factor encapsulation.

Additionally, it was found that impedance *in vivo*, although increasing immediately after implantation, was maintained at its initial value thereafter for the coated electrode, suggesting its great potential to be used as a biocompatible coating for chronic neural electrodes. Other recent advances in CP/hydrogel nanocomposite technology investigated the reduction of elasticity down to the range of 1–10 kPa to better mimic the mechanical properties of native brain tissue while preserving excellent electrical properties. In work done by Ding et al., polyaniline (PANI) was incorporated into photo-crosslinkable heparin-methacrylate hydrogels via *in situ* oxidative

polymerization (Figure 8J).^[287] The resulting polymer network exhibited impedance as low as 4.17 Ω and elastic moduli of around 1 kPa (Figure 8K). Other hydrogel-based nanocomposites, such as CNT^[106,285] or graphene-based^[286] hydrogel materials, although less frequently studied, represent important alternatives towards creating ideal neural interfaces. Although progress has been made, evaluations are still limited to *in vitro* or sub-chronic settings. Optimization of hydrogel-based composite materials still requires studies that examine the long-term performance of coated electrodes in a stimulated biological environment.

5. Conclusions and Future Perspectives

As highlighted in this review, applications of nanotechnology and nanomaterials in neural interfacing have the ability to produce stable long-term implants with improved electrical and mechanical properties. It is evident that the development of innovative diagnostic and therapeutic solutions to problems in neural medicine relies on improving neural electrodes and interfaces. For example, the ideal recording electrodes should be designed to have a small volume to minimize damage to the tissue, while maintaining high sensitivity, i.e., high SNR. However, it is nearly impossible to satisfy these competing requirements with conventional microfabrication methods and materials. It is believed that the nanotechnology fabrication methods discussed in this review could potentially overcome these limitations by producing electrodes with an extremely high surface to volume ratio, i.e., more probe units within the same volume, resulting in unprecedented specificity. Moreover, this review discussed how the development of specific nanomaterials is advancing neural interface engineering. Incorporation of the aforementioned carbon-based materials, CPs, and/or hybrid materials will lead to promising improvements in the performance of current neural electrodes based on their exceptional electronic, mechanical, and chemical properties. Bioelectronic transistors and electrodes such as CPs or hybrid materials have been further shown to improve long-term electrode viability and to reduce mechanical mismatches between natural neural tissue and neural implants as compared to plain metal electrodes.^[98,110–112,114,117,251,297,298]

Looking forward, several strategies could prove promising for the development of improved neural interfaces. First, the optimization of electrode geometrical properties, including size, volume, geometry, and surface morphology, have been shown to influence, in one way or another, biocompatibility and electrical properties of electrodes. These improvements could be achieved by adopting more advanced nanofabrication techniques and surface modification methods capable of producing electrodes deemed far less biologically invasive. Second, the development and employment of novel nanomaterials such as carbon-based materials, conducting polymers, hydrogels, and hybrid materials that possess superior physical properties and biocompatibility have the ability to overcome the limitations that conventional metallic and semimetal materials are facing, i.e., great mechanical mismatch and gliosis. Third, the delivery of pharmaceutical agents (such as anti-inflammatory drugs) and/or the incorporation of bioactive coatings that encourage

active neuron ingrowth may reduce reactive tissue responses and promote implant-tissue integration. In addition, chief among these trends is the development of wireless electrodes that enable prolonged recording and stimulation activities in the absence of bulky wires and attachments. Such technology could significantly improve our understanding of the brain by allowing continuous monitoring of neural signals during activities in which conventional wired electrodes would be prohibitive. Wireless electrodes could also enable the continuous stimulation of damaged or diseased brains to possibly restore functions of the CNS to people in need.

Additionally, researchers are incorporating natural materials within newly developed micro- and nanoelectrodes to improve biocompatibility for prolonged applications. For example, neural electrodes coated with extracellular matrix (ECM) proteins were shown to attenuate the foreign body response in the brain and to inhibit the inflammatory response. It is suggested that the incorporation of ECM proteins within electrodes can enhance cellular adhesion to the electrodes, enable efficient interfacial integration, and modulate organic activity.^[100] Experimental work is underway to address the challenges of low organic semiconductor carrier mobility, a shortage of data describing noise interference in organic transistors, and the lack of long-term in vivo studies characterizing the interfacial implant region.^[298] It is anticipated that advancements in these areas will lead to an improved ability to monitor, stimulate, and record neurophysiological signals. This in turn may enable a paradigm shift in the way that people with disorders of the CNS are diagnosed and treated.

Conflict of Interest

The authors declare no conflict of interest.

Keywords

nanofabrication, nanomaterials, neural electrodes, neural interfaces

Received: February 17, 2017

Revised: May 21, 2017

Published online:

- [1] K. Tudor, M. Tudor, L. Tudor, *Acta Med. Croat.* **2005**, 59, 307.
- [2] L. F. Haas, *J. Neurol. Neurosurg. Psychiatry* **2003**, 74, 7.
- [3] J. C. Sanchez, J. C. Principe, *Brain-Machine Interface Engineering*, 2, Morgan & Claypool Publishers, New York, **2007**.
- [4] K. Chapin, J. K. Moxon, *Neural Prostheses for Restoration of Sensory and Motor Function*, CRC Press, Boca Raton, **2001**.
- [5] E. Humayun, M. S. Weiland, J. D. Fujii, G. Y. Greenberg, R. Williamson, R. Little, J. Mech, B. Cimmarusti, V. Van Boemel, G. Dagnelie, G. de Juan, *Vis. Res* **2003**, 43, 2573.
- [6] T. W. Berger, M. Brandry, R. D. Brinton, J. Liaw, V. Z. Marmarelis, A. Park, B. J. Sheu, A. R. Tanguay, *Proc. IEEE* **2001**, 89, 993.
- [7] M. Lebedev, M. A. Crist, R. E. Nicolelis, *Methods for Neural Ensemble Recordings*, 2nd ed., CRC Press/Taylor&Francis, Boca Raton, **2008**.
- [8] K. Ohnishi, R. F. Weir, T. a. Kuiken, *Expert Rev. Med. Devices* **2007**, 4, 43.
- [9] G. Pfurtscheller, F. H. Lopes da Silva, *Clin. Neurophysiol.* **1999**, 110, 1842.
- [10] E. C. Leuthardt, G. Schalk, J. R. Wolpaw, J. G. Ojemann, D. W. Moran, *J. Neural Eng.* **2004**, 1, 63.
- [11] M. Nicolelis, *Methods for Neural Ensemble Recordings*, 1st ed., CRC Press, Boca Raton, **1999**.
- [12] J. Rickert, S. C. de Oliveira, E. Vaadia, A. Aertsen, S. Rotter, C. Mehring, *J. Neurosci.* **2005**, 25, 8815.
- [13] J. J. S. Norton, D. S. Lee, J. W. Lee, W. Lee, O. Kwon, P. Won, S.-Y. Jung, H. Cheng, J.-W. Jeong, A. Akce, S. Umunna, I. Na, Y. H. Kwon, X.-Q. Wang, Z. Liu, U. Paik, Y. Huang, T. Bretl, W.-H. Yeo, J. A. Rogers, *Proc. Natl. Acad. Sci. USA* **2015**, 112, 3920.
- [14] S. J. M. Smith, *J. Neurol. Neurosurg. Psychiatry* **2005**, 76, ii2.
- [15] M. Kutas, K. D. Federmeier, *Trends Cogn. Sci.* **2000**, 4, 463.
- [16] C. Babiloni, C. Del Percio, L. Arendt-Nielsen, A. Soricelli, G. L. Romani, P. M. Rossini, P. Capotosto, *Clin. Neurophysiol.* **2014**, 125, 1936.
- [17] J. R. Wolpaw, N. Birbaumer, D. J. McFarland, G. Pfurtscheller, T. M. Vaughan, *Clin. Neurophysiol.* **2002**, 113, 767.
- [18] N. Birbaumer, *Clinical Neurophysiology*. **2006**, 479.
- [19] M. D. Murphy, D. J. Guggenmos, D. T. Bundy, R. J. Nudo, *Front. Cell. Neurosci.* **2015**, 9, 497.
- [20] P. L. Nunez, R. Srinivasan, *Electric Fields of the Brain: The neurophysics of EEG*, Oxford University Press, Oxford, UK, **2009**.
- [21] M. S. Lewicki, *Network* **1998**, 9, R53.
- [22] M. E. Spira, A. Hai, *Nat. Nanotechnol.* **2013**, 8, 83.
- [23] Y. Fang, X. Li, Y. Fang, *J. Mater. Chem. C* **2015**, 3, 6424.
- [24] R. A. Green, P. B. Matteucci, R. T. Hassarati, B. Giraud, C. W. D. Dodds, S. Chen, P. J. Byrnes-Preston, G. J. Suaning, L. A. Poole-Warren, N. H. Lovell, *J. Neural Eng.* **2013**, 10, 16009.
- [25] L. Spataro, J. Dilgen, S. Retterer, A. J. Spence, M. Isaacson, J. N. Turner, W. Shain, *Exp. Neurol.* **2005**, 194, 289.
- [26] D. H. Szarowski, M. D. Andersen, S. Retterer, A. J. Spence, M. Isaacson, H. G. Craighead, J. N. Turner, W. Shain, *Brain Res.* **2003**, 983, 23.
- [27] L. Kam, W. Shain, J. N. Turner, R. Bizios, *Biomaterials* **1999**, 20, 2343.
- [28] J. N. Turner, W. Shain, D. H. Szarowski, M. Andersen, S. Martins, M. Isaacson, H. Craighead, *Exp. Neurol.* **1999**, 156, 33.
- [29] C. Chestek, V. Gilja, P. Nuyujukian, J. D. Foster, J. Fan, M. T. Kaufman, M. M. Churchland, Z. Rivera-Alvidrez, J. P. Cunningham, S. I. Ryu, K. V. Shenoy, *J. Neural Eng.* **2011**, 8, 45005.
- [30] A. Zjajo, *Brain-Machine Interface: Circuits and Systems*, Springer, Cham, Switzerland, **2016**.
- [31] J. T. W. Kuo, B. J. Kim, S. A. Hara, C. D. Lee, L. Yu, C. A. Gutierrez, T. Q. Hoang, V. Pikov, E. Meng, in *Proceedings of the IEEE International Conference on Micro Electro Mechanical Systems (MEMS)*, IEEE, Taipei, Taiwan, **2013**, pp. 1073.
- [32] W. Shen, L. Karumbaiah, X. Liu, T. Saxena, S. Chen, R. Patkar, R. V. Bellamkonda, M. G. Allen, *Microsystems Nanoeng.* **2015**, 1, 15010.
- [33] K. Lee, A. Singh, J. He, S. Massia, B. Kim, G. Raupp, *Sensors Actuators, B Chem.* **2004**, 102, 67.
- [34] DuPont, *Summary of Properties for Kapton Polyimide Films*, DuPont, Wilmington, DE, **1987**.
- [35] D. E. Arreaga-Salas, A. Avendaño-Bolívar, D. Simon, R. Reit, A. Garcia-Sandoval, R. L. Rennaker, W. Voit, *ACS Appl. Mater. Interfaces*, **2015**, 9, 26614.
- [36] A. Sridharan, J. K. Nguyen, J. R. Capadona, J. Muthuswamy, *J. Neural Eng.* **2015**, 12, 36002.
- [37] S. Kim, R. A. Normann, R. Harrison, F. Solzbacher, in *Annual International Conference of the IEEE Engineering in Medicine and Biology – Proceedings*, IEEE, New York, NY, **2006**, pp. 2986.
- [38] W. L. C. Rutten, *Annu. Rev. Biomed. Eng.* **2002**, 4, 407.

- [39] J. D. Bronzino, *Biomedical Engineering Fundamentals (The Biomedical Engineering Handbook, Third Edition)*, CRC Press, Florida, US **2006**.
- [40] E. Castagnola, A. Ansaldo, E. Maggolini, T. Ius, M. Skrap, D. Ricci, L. Fadiga, U. G. Hofmann, L. L. Furlanetti, *Front. Neuroeng.* **2014**, 7, 1.
- [41] S. G. Weber, *Anal. Chem.* **1989**, 61, 295.
- [42] P. Fattahi, G. Yang, G. Kim, M. R. Abidian, *Adv. Mater.* **2014**, 26, 1846.
- [43] D. McCreery, A. Lossinsky, V. Pikov, X. Liu, *IEEE Trans. Biomed. Eng.* **2006**, 53, 726.
- [44] Z. Zhao, R. Gong, H. Huang, J. Wang, *Sensors* **2016**, 16, 880.
- [45] J. Song, L. Wang, A. Zibart, C. Koch, *Metals* **2012**, 2, 450.
- [46] K. Seidl, M. Schwaerzle, I. Ulbert, H. P. Neves, O. Paul, P. Ruther, *J. Microelectromechanical Syst.* **2012**, 21, 1426.
- [47] J. Du, M. L. Roukes, S. C. Masmanidis, *J. Micromechanics Micro-engineering* **2009**, 19, 75008.
- [48] M. T. B. Toossi, F. Akbari, S. Bayani, A. Jafari, M. Malakzadeh, in *World Congress on Medical Physics & Biomedical Engineering*, (Eds: O. Dössel, W. C. Schlegel), Springer, Munich, Germany **2009**, 89.
- [49] C. Henle, M. Raab, J. G. Cordeiro, S. Doostkam, A. Schulze-Bonhage, T. Stieglitz, J. Rickert, *Biomed. Microdevices* **2011**, 13, 59.
- [50] J. S. Ordonez, V. Pikov, H. Wiggins, C. Patten, T. Stieglitz, J. Rickert, M. Schuettler, in *Engineering in Medicine and Biology Society (EMBC), 2014 36th Annual Int. Conf. of the IEEE, IEEE, Chicago, IL* **2014**, 6846.
- [51] C. M. Lewandowski, N. Co-investigator, C. M. Lewandowski, *Towards Practical Brain-Computer Interfaces: Bridging the Gap from Research to Real-World Applications, Biological and Medical Physics, Biomedical Engineering*, Vol. 1, Springer-Verlag Berlin Heidelberg, Germany, **2015**.
- [52] M. Schuettler, S. Stiess, B. V. King, G. J. Suaning, *J. Neural Eng.* **2005**, 2, S121.
- [53] C. Henle, C. Hassler, F. Kohler, M. Schuettler, T. Stieglitz, in *Proceedings of the Annual Int. Conf. of the IEEE Engineering in Medicine and Biology Society, EMBS, IEEE, Boston, MA*, **2011**, 640.
- [54] M. Schuettler, D. Pfau, J. S. Ordonez, C. Henle, P. Woias, T. Stieglitz, in *Proceedings of the 31st Annual Int. Conf. of the IEEE Engineering in Medicine and Biology Society: Engineering the Future of Biomedicine, EMBC 2009, IEEE, Minneapolis, MN*, **2009**, 1612.
- [55] M. Schuettler, C. Henle, J. Ordonez, G. J. Suaning, N. H. Lovell, T. Stieglitz, in *Proceedings of the 3rd Int. IEEE EMBS Conf. on Neural Engineering, IEEE, Piscataway, NJ*, **2007**, 53.
- [56] F. Kohler, M. Schuettler, T. Stieglitz, in *Proceedings of the Annual Int. Conf. of the IEEE Engineering in Medicine and Biology Society, EMBS, IEEE, Piscataway, NJ*, **2012**, 5130.
- [57] N. H. Rizvi, *Glass* **2003**, 50, 107.
- [58] R. R. Gattass, E. Mazur, *Nat. Photonics* **2008**, 2, 219.
- [59] J. Qiu, K. Miura, K. Hirao, *J. Non. Cryst. Solids* **2008**, 354, 1100.
- [60] A. Ovsianikov, A. Ostendorf, B. N. Chichkov, *Appl. Surf. Sci.* **2007**, 253, 6599.
- [61] H. Misawa, H.-B. Sun, S. Juodkakis, M. Watanabe, S. Matsuo, in *Proceedings of SPIE – The International Society for Optical Engineering*, SPIE Digital Library, **2000**.
- [62] S. Ameer-Beg, W. Perrie, S. Rathbone, J. Wright, W. Weaver, H. Champoux, *Appl. Surf. Sci.* **1998**, 127–129, 875.
- [63] S. Nolte, C. Momm, H. Jacobs, A. Tu, B. N. Chichkov, B. Welleghausen, H. Welling, *J. Opt. Soc. Am. B* **1997**, 14, 2716.
- [64] K. C. Cheung, *Biomed. Microdevices* **2007**, 9, 923.
- [65] K. D. Wise, *IEEE Eng. Med. Biol. Mag.* **2005**, 24, 22.
- [66] K. D. Wise, J. B. Angell, *IEEE Trans. Biomed. Eng.* **1975**, BME-22, 212.
- [67] T. Stieglitz, in *Microsystem Technologies*, 16, Springer-Verlag Berlin Heidelberg, Germany, **2010**, pp. 723–734.
- [68] A. C. Patil, N. V. Thakor, *Med. Biol. Eng. Comput.* **2016**, 54, 23.
- [69] L. R. Hochberg, M. D. Serruya, G. M. Friebs, J. A. Mukand, M. Saleh, A. H. Caplan, A. Branner, D. Chen, R. D. Penn, J. P. Donoghue, *Nature* **2006**, 442, 164.
- [70] S. Kim, R. Bhandari, M. Klein, S. Negi, L. Rieth, P. Tathireddy, M. Toepfer, H. Oppermann, F. Solzbacher, *Biomed. Microdevices* **2009**, 11, 453.
- [71] N. A. Kotov, J. O. Winter, I. P. Clements, E. Jan, B. P. Timko, S. Campidelli, S. Pathak, A. Mazzatenta, C. M. Lieber, M. Prato, R. V. Bellamkonda, G. A. Silva, N. W. S. Kam, F. Patolsky, L. Ballerini, *Adv. Mater.* **2009**, 21, 3970.
- [72] A. E. Grigorescu, C. W. Hagen, *Nanotechnology* **2009**, 20, 31.
- [73] M. Manheller, S. Trellenkamp, R. Waser, S. Karthäuser, *Nanotechnology* **2012**, 23, 125302.
- [74] A. Errachid, C. A. Mills, M. Pla-Roca, M. J. Lopez, G. Villanueva, J. Bausells, E. Crespo, F. Teixidor, J. Samitier, *Mater. Sci. Eng. C* **2008**, 28, 777.
- [75] P. S. Ali Eftekhari, R. C. Alkire, Y. Gogotsi, *Nanostructured Materials in Electrochemistry*, Wiley-VCH Verlag GmbH & Co., Weinheim, Germany, **2008**.
- [76] F. Watt, A. A. Bettiol, J. A. Van Kan, E. J. Teo, M. B. H. Breese, *Int. J. Nanosci.* **2005**, 4, 269.
- [77] S. T. Kelly, J. C. Trenkle, L. J. Koerner, S. C. Barron, N. Walker, P. O. Pouliquen, M. W. Tate, S. M. Gruner, E. M. Dufresne, T. P. Weihs, T. C. Hufnagel, *J. Synchrotron Radiat.* **2011**, 18, 464.
- [78] P. Steinmann, J. M. R. Weaver, *J. Vac. Sci. Technol. B* **2004**, 22, 3178.
- [79] K. Liu, P. Avouris, J. Bucchignano, R. Martel, S. Sun, J. Michl, *Appl. Phys. Lett.* **2002**, 80, 865.
- [80] X. Cui, J. F. Hetke, J. A. Wiler, D. J. Anderson, D. C. Martin, *Sensors Actuators A Phys.* **2001**, 93, 8.
- [81] J. M. Fonner, L. Forciniti, H. Nguyen, J. D. Byrne, Y.-F. Kou, J. Syeda-Nawaz, C. E. Schmidt, *Biomed. Mater.* **2008**, 3, 34124.
- [82] E. Castagnola, L. Maiolo, E. Maggolini, A. Minotti, M. Marrani, F. Maita, A. Pecora, G. N. Angotzi, A. Ansaldo, M. Boffini, L. Fadiga, G. Fortunato, D. Ricci, in *IEEE Transactions on Neural Systems and Rehabilitation Engineering*, IEEE, Piscataway, NJ **2015**, 23, 342.
- [83] X. Luo, C. L. Weaver, D. D. Zhou, R. Greenberg, X. T. Cui, *Biomaterials* **2011**, 32, 5551.
- [84] Y. Xiao, C. M. Li, S. Yu, Q. Zhou, V. S. Lee, S. M. Mochhala, *Talanta* **2007**, 72, 532.
- [85] E. Jan, J. L. Hendricks, V. Husaini, S. M. Richardson-Burns, A. Sereno, D. C. Martin, N. A. Kotov, *Nano Lett.* **2009**, 9, 4012.
- [86] X. Wang, H. Zhu, Y. Xu, H. Wang, Y. Tao, S. Hark, X. Xiao, Q. Li, *ACS Nano*, **2010**, 4, 3302.
- [87] C. Subramaniam, A. Sekiguchi, T. Yamada, D. N. Futaba, K. Hata, *Nanoscale* **2016**, 8, 3888.
- [88] F. Béguin, E. Fr ckowiak, *Carbons for Electrochemical Energy Storage and Conversion Systems*, 1, CRC Press, Boca Raton, FL, **2009**.
- [89] Y. J. Lee, D. J. Park, J. Y. Park, Y. Kim, *Sensors* **2008**, 8, 6154.
- [90] F. Chen, Q. Qing, L. Ren, Z. Wu, Z. Liu, *Appl. Phys. Lett.* **2005**, 86, 1.
- [91] H. Park, a. K. L. Lim, a. P. Alivisatos, J. Park, P. L. McEuen, *Appl. Phys. Lett.* **1999**, 75, 301.
- [92] X. Tian, J. Li, D. Xu, *Electrochem. Commun.* **2010**, 12, 1081.
- [93] X. Geng, E. J. Podlaha, *Nano Lett.* **2016**, 16, 7439.
- [94] P. Shi, P. W. Bohn, *ACS Nano* **2008**, 2, 1581.
- [95] Z. Spitalsky, D. Tasis, K. Papagelis, C. Galiotis, *Prog. Polym. Sci.* **2010**, 35, 357.
- [96] G. Baranauskas, E. Maggolini, E. Castagnola, A. Ansaldo, A. Mazzoni, G. N. Angotzi, A. Vato, D. Ricci, S. Panzeri, L. Fadiga, *J. Neural Eng.* **2011**, 8, 66013.
- [97] T. Gabay, M. Ben-David, I. Kalifa, R. Sorkin, Z. R. Abrams, E. Ben-Jacob, Y. Hanein, *Nanotechnology* **2007**, 18, 35201.

- [98] E. W. Keefer, B. R. Botterman, M. I. Romero, A. F. Rossi, G. W. Gross, *Nat. Nanotechnol.* **2008**, *3*, 434.
- [99] H. Luo, Z. Shi, N. Li, Z. Gu, Q. Zhuang, *Anal. Chem.* **2001**, *73*, 915.
- [100] E. Ben-Jacob, Y. Hanein, *J. Mater. Chem.* **2008**, *18*, 5181.
- [101] N. R. Franklin, Q. Wang, T. W. Tomblor, A. Javey, M. Shim, H. Dai, *Appl. Phys. Lett.* **2002**, *81*, 913.
- [102] L. H. Hess, M. Jansen, V. Maybeck, M. V. Hauf, M. Seifert, M. Stutzmann, I. D. Sharp, A. Offenhäusser, J. A. Garrido, *Adv. Mater.* **2011**, *23*, 5045.
- [103] J. J. Pancrazio, *Nanomedicine* **2008**, *3*, 823.
- [104] K. Wang, H. A. H. a. Fishman, H. Dai, J. S. J. S. Harris, *Nano Lett.* **2006**, *6*, 2043.
- [105] G. W. Gross, W. Y. Wen, J. W. Lin, *J. Neurosci. Methods* **1985**, *15*, 243.
- [106] L. He, D. Lin, Y. Wang, Y. Xiao, J. Che, *Colloids Surfaces B Biointerfaces* **2011**, *87*, 273.
- [107] N. A. Alba, Z. J. Du, K. A. Catt, T. D. Y. Kozai, X. T. Cui, *Biosensors* **2015**, *5*, 618.
- [108] M. Gerard, A. Chaubey, B. D. Malhotra, *Biosens. Bioelectron.* **2002**, *17*, 345.
- [109] G. A. Snook, P. Kao, A. S. Best, *J. Power Sources* **2011**, *196*, 1.
- [110] U. A. Aregueta-Robles, A. J. Woolley, L. A. Poole-Warren, N. H. Lovell, R. A. Green, *Front. Neuroeng.* **2014**, *7*, 15.
- [111] Z. Nie, E. Kumacheva, *Nat. Mater.* **2008**, *7*, 277.
- [112] D. Ho, J. Zou, X. Chen, A. Munshi, N. M. Smith, V. Agarwal, S. I. Hodgetts, G. W. Plant, A. J. Bakker, A. R. Harvey, I. Luzinov, K. S. Iyer, *ACS Nano* **2015**, *9*, 1767.
- [113] N. K. Guimard, N. Gomez, C. E. Schmidt, *Prog. Polym. Sci.* **2007**, *32*, 876.
- [114] A. Gelmi, M. K. Ljunggren, M. Rafat, E. W. H. Jager, *J. Mater. Chem. B* **2014**, *2*, 3860.
- [115] M. R. Abidian, D.-H. Kim, D. C. Martin, *Adv. Mater.* **2006**, *18*, 405.
- [116] D. T. Simon, E. O. Gabrielson, K. Tybrandt, M. Berggren, *Chem. Rev.* **2016**, *116*, 13009.
- [117] U. Lange, N. V. Roznyatovskaya, V. M. Mirsky, *Anal. Chim. Acta* **2008**, *614*, 1.
- [118] S. F. Cogan, *Annu. Rev. Biomed. Eng.* **2008**, *10*, 275.
- [119] M. Jorfi, J. L. Skousen, C. Weder, J. R. Capadona, *J. Neural Eng.* **2015**, *12*, 11001.
- [120] D. R. Merrill, *Implantable Neural Prosthesis 2: Techniques and Engineering Approaches*, Springer, New York, **2010**, Ch. 4, pp. 85–138.
- [121] D. R. Merrill, M. Bikson, J. G. R. Jefferys, *J. Neurosci. Methods* **2005**, *141*, 171.
- [122] X. Cui, D. C. Martin, *Sensors Actuators B Chem.* **2003**, *89*, 92.
- [123] W. F. Agnew, D. B. McCreery, T. G. H. Yuen, L. A. Bullara, in *Neural Prosthesis: Fundamental Studies*, (Eds: W. Agnew, D. McCreery), Prentice Hall, Englewood Cliffs, NJ, **1990**, pp. 225–252.
- [124] S. S. Stensaas, L. J. Stensaas, *Acta Neuropathol.* **1978**, *41*, 145.
- [125] A. M. Dymond, L. E. Kaechele, J. M. Jurist, P. H. Crandall, *J. Neurosurg.* **1970**, *33*, 574.
- [126] R. G. Bickford, G. Fischer, G. P. Sayre, *Proc. Staff Meet. Mayo Clin.* **1957**, *32*, 14.
- [127] M. R. Abidian, D. C. Martin, *Adv. Funct. Mater.* **2009**, *19*, 573.
- [128] X. Cui, J. Wiler, M. Dzaman, R. A. Altschuler, D. C. Martin, *Biomaterials* **2003**, *24*, 777.
- [129] R. A. Green, N. H. Lovell, G. G. Wallace, L. A. Poole-Warren, *Biomaterials* **2008**, *29*, 3393.
- [130] L. A. Geddes, R. Roeder, *Ann. Biomed. Eng.* **2003**, *31*, 879.
- [131] S. Negi, R. Bhandari, F. Solzbacher, *J. Sens. Technol.* **2012**, *2*, 138.
- [132] S. F. Cogan, P. R. Troyk, J. Ehrlich, C. M. Gasbarro, T. D. Plante, *J. Neural Eng.* **2007**, *4*, 79.
- [133] H. Shi, J. I. Yeh, *Nanomedicine* **2007**, *2*, 587.
- [134] H. Shi, T. Xia, A. E. Nel, J. I. Yeh, *Nanomedicine* **2007**, *2*, 599.
- [135] R. M. Penner, M. J. Heben, T. L. Longin, N. S. Lewis, *Science* **1990**, *250*, 1118.
- [136] M. V. Mirkin, F.-R. F. Fan, A. J. Bard, *J. Electroanal. Chem.* **1992**, *328*, 47.
- [137] G. T. A. Kovacs, in *Enabling technologies for cultured neural networks*, (Eds: D. A. Stenger, T. McKenna), Academic Press, Cambridge, MA, **1994**, pp. 121–165.
- [138] N. A. Kotov, J. O. Winter, I. P. Clements, E. Jan, B. P. Timko, S. Campidelli, S. Pathak, A. Mazzatenta, C. M. Lieber, M. Prato, R. V. Bellamkonda, G. A. Silva, N. W. S. Kam, F. Patolsky, L. Ballerini, *Adv. Mater.* **2009**, *21*, 3970.
- [139] C. Vallejo-Giraldo, A. Kelly, M. J. P. Biggs, *Drug Discovery Today* **2014**, *19*, 88.
- [140] N. V. Apollo, M. I. Maturana, W. Tong, D. A. X. Nayagam, M. N. Shivdasani, J. Foroughi, G. G. Wallace, S. Prawer, M. R. Ibbotson, D. J. Garrett, *Adv. Funct. Mater.* **2015**, *25*, 3551.
- [141] V. C. Sanchez, A. Jachak, R. H. Hurt, A. B. Kane, *Chem. Res. Toxicol.* **2012**, *25*, 15.
- [142] X. Dong, Y. Shi, W. Huang, P. Chen, L.-J. Li, *Adv. Mater.* **2010**, *22*, 1649.
- [143] H. Y. Mao, S. Laurent, W. Chen, O. Akhavan, M. Imani, A. A. Ashkarran, M. Mahmoudi, *Chem. Rev.* **2013**, *113*, 3407.
- [144] Y. Shao, J. Wang, H. Wu, J. Liu, I. A. Aksay, Y. Lin, *Electroanalysis* **2010**, *22*, 1027.
- [145] C. Lee, X. Wei, J. W. Kysar, J. Hone, *Science* **2008**, *321*, 385.
- [146] S. Stankovich, D. A. Dikin, G. H. B. Dommett, K. M. Kohlhaas, E. J. Zimney, E. A. Stach, R. D. Piner, S. T. Nguyen, R. S. Ruoff, *Nature* **2006**, *442*, 282.
- [147] C. Chiu, X. He, H. Liang, *Electrochim. Acta* **2013**, *94*, 42.
- [148] E. Pérez, M. P. Lichtenstein, C. Suñol, N. Casañ-Pastor, *Mater. Sci. Eng. C* **2015**, *55*, 218.
- [149] F. Li, J. Li, Y. Feng, L. Yang, Z. Du, *Sensors Actuators, B Chem.* **2011**, *157*, 110.
- [150] L. J. Cote, F. Kim, J. Huang, *J. Am. Chem. Soc.* **2009**, *131*, 1043.
- [151] X. Zuo, S. He, D. Li, C. Peng, Q. Huang, S. Song, C. Fan, *Langmuir* **2010**, *26*, 1936.
- [152] Z. Singh, *Nanotechnol. Sci. Appl.* **2016**, *9*, 15.
- [153] Y. Chang, S.-T. Yang, J.-H. Liu, E. Dong, Y. Wang, A. Cao, Y. Liu, H. Wang, *Toxicol. Lett.* **2011**, *200*, 201.
- [154] P. K. Nayak, in *Recent Advances in Graphene Research*, InTech, Croatia, **2016**.
- [155] L. Tang, Y. Wang, Y. Li, H. Feng, J. Lu, J. Li, *Adv. Funct. Mater.* **2009**, *19*, 2782.
- [156] M. Zhou, Y. Zhai, S. Dong, *Anal. Chem.* **2009**, *81*, 5603.
- [157] S. Jia, H. D. Sun, J. H. Du, Z. K. Zhang, D. D. Zhang, L. P. Ma, J. S. Chen, D. G. Ma, H. M. Cheng, W. C. Ren, *Nanoscale* **2016**, *8*, 10714.
- [158] Y. Lu, H. Lyu, A. G. Richardson, T. H. Lucas, D. Kuzum, *Sci. Rep.* **2016**, *6*, 33526.
- [159] Z. Peng, J. Lin, R. Ye, E. L. G. Samuel, J. M. Tour, *ACS Appl. Mater. Interfaces* **2015**, *7*, 3414.
- [160] D.-W. Park, A. A. Schendel, S. Mikael, S. K. Brodnick, T. J. Richner, J. P. Ness, M. R. Hayat, F. Atry, S. T. Frye, R. Pashaie, S. Thongpang, Z. Ma, J. C. Williams, *Nat. Commun.* **2014**, *5*, 5258.
- [161] S. Bae, H. Kim, Y. Lee, X. Xu, J.-S. Park, Y. Zheng, J. Balakrishnan, T. Lei, H. Ri Kim, Y. Il Song, Y.-J. Kim, K. S. Kim, B. Özyilmaz, J.-H. Ahn, B. H. Hong, S. Iijima, *Nat. Nanotechnol.* **2010**, *5*, 574.
- [162] L. A. Bullara, D. B. McCreery, T. G. Yuen, W. F. Agnew, *J. Neurosci. Methods* **1983**, *9*, 15.
- [163] S. Agarwal, X. Zhou, F. Ye, Q. He, G. C. K. Chen, J. Soo, F. Boey, H. Zhang, P. Chen, *Langmuir* **2010**, *26*, 2244.
- [164] C. Lee, X. Wei, J. W. Kysar, J. Hone, *Science* **2008**, *321*, 385.
- [165] M.-F. Yu, B. S. Files, S. Arepalli, R. S. Ruoff, *Phys. Rev. Lett.* **2000**, *84*, 5552.
- [166] M.-F. Yu, O. Lourie, M. J. Dyer, K. Moloni, T. F. Kelly, R. S. Ruoff, *Science* **2000**, *287*, 637.

- [167] Y. Zhang, S. F. Ali, E. Dervishi, Y. Xu, Z. Li, D. Casciano, A. S. Biris, *ACS Nano* **2010**, *4*, 3181.
- [168] J. Yi, Z. Zhao, S. Li, Y. Yin, X. Wang, *J. Wuhan Univ. Technol. Sci. Ed.* **2016**, *31*, 925.
- [169] A. Fabbro, D. Scaini, V. León, E. Vázquez, G. Cellot, G. Privitera, L. Lombardi, F. Torrisi, F. Tomarchio, F. Bonaccorso, S. Bosi, A. C. Ferrari, L. Ballerini, M. Prato, *ACS Nano* **2016**, *10*, 615.
- [170] V. C. Moser, *Toxicol. Pathol.* **2011**, *39*, 36.
- [171] M. C. P. Mendonca, E. S. Soares, M. B. de Jesus, H. J. Ceragioli, S. P. Irazusta, A. G. Batista, M. A. R. Vinolo, M. R. Marostica Junior, M. A. da Cruz-Hofling, *J. Nanobiotechnology* **2016**, *14*, 53.
- [172] S. Iijima, *Nature* **1991**, *354*, 56.
- [173] J. W. G. Wilder, L. C. Venema, A. G. Rinzler, R. E. Smalley, C. Dekker, *Nature* **1998**, *391*, 59.
- [174] J.-C. Charlier, X. Blase, S. Roche, *Rev. Mod. Phys.* **2007**, *79*, 677.
- [175] A. M. Monaco, M. Giugliano, *Beilstein J. Nanotechnol.* **2014**, *5*, 1849.
- [176] Z. Chen, Z. Wu, L. Tong, H. Pan, Z. Liu, *Anal. Chem.* **2006**, *78*, 8069.
- [177] A. V. Patil, A. F. Beker, F. G. M. Wiertz, H. A. Heering, G. Coslovich, R. Vlijm, T. H. Oosterkamp, *Nanoscale* **2010**, *2*, 734.
- [178] Y. Fan, C. Han, B. Zhang, *Analyst* **2016**, *141*, 5474.
- [179] L. Zhang, T. J. Webster, *Nano Today* **2009**, *4*, 66.
- [180] A. Nunes, K. Al-Jamal, T. Nakajima, M. Hariz, K. Kostarelos, *Arch. Toxicol.* **2012**, *86*, 1009.
- [181] E. W. Keefer, B. R. Botterman, M. I. Romero, A. F. Rossi, G. W. Gross, *Nat. Nanotechnol.* **2008**, *3*, 434.
- [182] R.-S. Chen, W.-H. Huang, H. Tong, A. Zong-Li Wang, J.-K. Cheng, *Anal. Chem.*, **2003**, *75*, 6341.
- [183] D. B. McCreery, W. F. Agnew, T. G. Yuen, L. Bullara, *IEEE Trans. Biomed. Eng.* **1990**, *37*, 996.
- [184] D. R. Merrill, M. Bikson, J. G. R. Jefferys, *J. Neurosci. Methods* **2005**, *141*, 171.
- [185] S. B. Brummer, L. S. Robblee, F. T. Hambrecht, *Ann. N. Y. Acad. Sci.* **1983**, *405*, 159.
- [186] S. F. Cogan, T. D. Plante, J. Ehrlich, A. Smirnov, D. B. Shire, M. Gingerich, J. F. Rizzo, *J. Biomed. Mater. Res., Part B* **2009**, *89B*, 353.
- [187] T. S. Phely Bobin, T. Tiano, B. Farrell, R. Fooksa, L. Robblee, D. J. Edell, R. Czerw, *MRS Proc.* **2006**, *926*, 926.
- [188] V. Georgakilas, K. Kordatos, M. Prato, D. M. Guldi, M. Holzinger, A. Hirsch, *J. Am. Chem. Soc.* **2002**, *124*, 760.
- [189] A. Bianco, K. Kostarelos, M. Prato, *Chem. Commun.* **2011**, *47*, 10182.
- [190] Y.-P. Sun, K. Fu, Y. Lin, W. Huang, *Acc. Chem. Res.* **2002**, *35*, 1096.
- [191] R. H. Baughman, A. A. Zakhidov, W. A. de Heer, *Science* **2002**, *297*, 787.
- [192] M. P. Mattson, R. C. Haddon, A. M. Rao, *J. Mol. Neurosci.* **2000**, *14*, 175.
- [193] K. Donaldson, R. Aitken, L. Tran, V. Stone, R. Duffin, G. Forrest, A. Alexander, *Toxicol. Sci.* **2006**, *92*, 5.
- [194] V. Lovat, D. Pantarotto, L. Lagostena, B. Cacciari, M. Grandolfo, M. Righi, G. Spalluto, M. Prato, L. Ballerini, *Nano Lett.* **2005**, *5*, 1107.
- [195] M. Zheng, A. Jagota, E. D. Semke, B. A. Diner, R. S. Mclean, S. R. Lustig, R. E. Richardson, N. G. Tassi, *Nat. Mater.* **2003**, *2*, 338.
- [196] G. R. Dieckmann, A. B. Dalton, P. A. Johnson, J. Razal, J. Chen, G. M. Giordano, E. Muñoz, I. H. Musselman, R. H. Baughman, R. K. Draper, *J. Am. Chem. Soc.*, **2003**, *125*, 1770.
- [197] R. Shvartzman-Cohen, Y. Levi-Kalishman, E. Nativ-Roth, R. Yerushalmi-Rozen, *Langmuir*, **2004**, *20*, 6085.
- [198] V. C. Moore, M. S. Strano, E. H. Haroz, R. H. Hauge, R. E. Smalley, J. Schmidt, Y. Talmon, *Nano Lett.*, **2003**, *3*, 1380.
- [199] A. V. Liopo, M. P. Stewart, J. Hudson, J. M. Tour, T. C. Pappas, *J. Nanosci. Nanotechnol.* **2006**, *6*, 1365.
- [200] M. S. Strano, C. A. Dyke, M. L. Usrey, P. W. Barone, M. J. Allen, H. Shan, C. Kittrell, R. H. Hauge, J. M. Tour, R. E. Smalley, *Science* **2003**, *301*, 1519.
- [201] M. Shim, N. W. S. Kam, R. J. Chen, Y. Li, H. Dai, *Nano Lett.*, **2002**, *2*, 285.
- [202] J. Shen, W. Wang, Q. Chen, M. Wang, S. Xu, Y. Zhou, X.-X. Zhang, *Nanotechnology* **2009**, *20*, 245307.
- [203] I. Heller, J. Kong, H. A. Heering, K. A. Williams, S. G. Lemay, C. Dekker, *Nano Lett.* **2005**, *5*, 137.
- [204] Y. Lu, T. Li, X. Zhao, M. Li, Y. Cao, H. Yang, Y. Y. Duan, *Biomaterials* **2010**, *31*, 5169.
- [205] T. Gabay, M. Ben-David, I. Kalifa, R. Sorkin, Z. R. Abrams, E. Ben-Jacob, Y. Hanein, *Nanotechnology* **2007**, *18*, 35201.
- [206] T. E. McKnight, M. N. Ericson, S. W. Jones, A. V. Melechko, M. L. Simpson, in *Engineering in Medicine and Biology Society, 2007. EMBS 2007. 29th Annual International Conference of the IEEE*, IEEE, Lyon, France **2007**, 5381.
- [207] S. Miserendino, J. Yoo, A. Cassell, Y.-C. Tai, *Nanotechnology* **2006**, *17*, S23.
- [208] L. Bareket, N. Waiskopf, D. Rand, G. Lubin, M. David-Pur, J. Ben-Dov, S. Roy, C. Eleftheriou, E. Sernagor, O. Cheshnovsky, U. Banin, Y. Hanein, *Nano Lett.* **2014**, *14*, 6685.
- [209] A. Fabbro, M. Prato, L. Ballerini, *Adv. Drug Deliv. Rev.* **2013**, *65*, 2034.
- [210] S. Kruss, A. J. Hilmer, J. Zhang, N. F. Reuel, B. Mu, M. S. Strano, *Adv. Drug Deliv. Rev.* **2013**, *65*, 1933.
- [211] G. Baranauskas, E. Maggiolini, E. Castagnola, A. Ansaldo, A. Mazzoni, G. N. Angotzi, A. Vato, D. Ricci, S. Panzeri, L. Fadiga, *J. Neural Eng.* **2011**, *8*, 66013.
- [212] M. P. Mattson, R. C. Haddon, A. M. Rao, *J. Mol. Neurosci.* **2000**, *14*, 175.
- [213] Y. Lu, T. Li, X. Zhao, M. Li, Y. Cao, H. Yang, Y. Y. Duan, *Biomaterials* **2010**, *31*, 5169.
- [214] U. A. Aregueta-Robles, A. J. Woolley, L. A. Poole-Warren, N. H. Lovell, R. A. Green, *Front. Neuroeng.* **2014**, *7*, 15.
- [215] R. Balint, N. J. Cassidy, S. H. Cartmell, *Acta Biomater.* **2014**, *10*, 2341.
- [216] M. R. Abidian, J. M. Corey, D. R. Kipke, D. C. Martin, *Small* **2010**, *6*, 421.
- [217] H. Yamato, M. Ohwa, W. Wernet, *J. Electroanal. Chem.* **1995**, *397*, 163.
- [218] R. A. Green, L. A. Poole-Warren, N. H. Lovell, in *2007 3rd Int. IEEE/EMBS Conf. on Neural Engineering*, IEEE, Lyon, France, **2007**, pp. 97–100.
- [219] H. Zhou, X. Cheng, L. Rao, T. Li, Y. Y. Duan, *Acta Biomater.* **2013**, *9*, 6439.
- [220] J.-W. Jeong, G. Shin, S. I. Park, K. J. Yu, L. Xu, J. A. Rogers, *Neuron* **2015**, *86*, 175.
- [221] P. Murray, G. M. Spinks, G. G. Wallace, R. P. Burford, *Synth. Met.* **1997**, *84*, 847.
- [222] J. Yang, D. C. Martin, *J. Mater. Res.* **2006**, *21*, 1124.
- [223] S. Baek, R. A. Green, L. A. Poole-Warren, *J. Biomed. Mater. Res. Part A* **2014**, *102*, 2743.
- [224] T. Someya, Z. Bao, G. G. Malliaras, *Nature* **2016**, *540*, 379.
- [225] D. E. Discher, P. Janmey, Y. Wang, *Science* **2005**, *310*, 1139.
- [226] L. Ouyang, C. L. Shaw, C.-C. Kuo, A. L. Griffin, D. C. Martin, *J. Neural Eng.* **2014**, *11*, 26005.
- [227] S. J. Wilks, A. J. Woolley, L. Ouyang, D. C. Martin, K. J. Otto, in *2011 Annual Int. Conf. of the IEEE Engineering in Medicine and Biology Society*, IEEE, Piscataway, NJ, **2011**, pp. 5412–5415.
- [228] R. A. Green, R. T. Hassarati, L. Bouchinet, C. S. Lee, G. L. M. Cheong, J. F. Yu, C. W. Dodds, G. J. Suaning, L. A. Poole-Warren, N. H. Lovell, *Biomaterials* **2012**, *33*, 5875.

- [229] X. Cui, D. C. Martin, *Sensors Actuators A Phys.* **2003**, *103*, 384.
- [230] B. Wei, J. Liu, L. Ouyang, C.-C. Kuo, D. C. Martin, *ACS Appl. Mater. Interfaces* **2015**, *7*, 15388.
- [231] S. Kim, L. K. Jang, H. S. Park, J. Y. Lee, *Sci. Rep.* **2016**, *6*, 30475.
- [232] J. Y. Wong, R. Langer, D. E. Ingber, *Proc. Natl. Acad. Sci. USA* **1994**, *91*, 3201.
- [233] C. E. Schmidt, V. R. Shastri, J. P. Vacanti, R. Langer, *Proc. Natl. Acad. Sci. USA* **1997**, *94*, 8948.
- [234] A. Kotwal, C. E. Schmidt, *Biomaterials* **2001**, *22*, 1055.
- [235] C. Saltó, E. Saindon, M. Bolin, A. Kanciużewska, M. Fahlman, E. W. H. Jager, P. Tengvall, E. Arenas, M. Berggren, *Langmuir* **2008**, *24*, 14133.
- [236] A. M. D. Wan, D. J. Brooks, A. Gumus, C. Fischbach, G. G. Malliaras, *Chem. Commun.* **2009**, 279, 5278.
- [237] M. H. Bolin, K. Svennersten, D. Nilsson, A. Sawatdee, E. W. H. Jager, A. Richter-Dahlfors, M. Berggren, *Adv. Mater.* **2009**, *21*, 4379.
- [238] A. M. D. Wan, R. M. Schur, C. K. Ober, C. Fischbach, D. Gourdon, G. G. Malliaras, *Adv. Mater.* **2012**, *24*, 2501.
- [239] M. P. Lutolf, J. A. Hubbell, *Nat. Biotechnol.* **2005**, *23*, 47.
- [240] M. J. Mahoney, W. M. Saltzman, *Nat. Biotechnol.* **2001**, *19*, 934.
- [241] E. De Giglio, L. Sabbatini, S. Colucci, G. Zamboni, *J. Biomater. Sci. Polym. Ed.* **2000**, *11*, 1073.
- [242] L. K. Povlich, J. C. Cho, M. K. Leach, J. M. Corey, J. Kim, D. C. Martin, *Biochim. Biophys. Acta – Gen. Subj.* **2013**, *1830*, 4288.
- [243] B. Zhu, S.-C. Luo, H. Zhao, H.-A. Lin, J. Sekine, A. Nakao, C. Chen, Y. Yamashita, H. Yu, *Nat. Commun.* **2014**, *5*, 1065.
- [244] X. Liu, Z. Yue, M. J. Higgins, G. G. Wallace, *Biomaterials* **2011**, *32*, 7309.
- [245] N. Gomez, C. E. Schmidt, *J. Biomed. Mater. Res. Part A* **2007**, *81A*, 135.
- [246] J. Y. Lee, J.-W. Lee, C. E. Schmidt, *J. R. Soc. Interface* **2009**, *6*.
- [247] B. C. Thompson, S. E. Moulton, R. T. Richardson, G. G. Wallace, *Biomaterials* **2011**, *32*, 3822.
- [248] U. G. Hofmann, J. Krüger, *Front. Neuroeng.* **2015**, *8*, 3.
- [249] R. Wadhwa, C. F. Lagenaur, X. T. Cui, *J. Control. Release* **2006**, *110*, 531.
- [250] S. Sirivisoot, R. Pareta, T. J. Webster, *Nanotechnology* **2011**, *22*, 85101.
- [251] N. Guimard, N. Gomez, C. Schmidt, *Prog. Polym. Sci.* **2007**, *32*, 876.
- [252] A. Krishnan, E. Dujardin, T. W. Ebbesen, P. N. Yianilos, M. M. J. Treacy, *Phys. Rev. B* **1998**, *58*, 14013.
- [253] S. K. Seidlits, J. Y. Lee, C. E. Schmidt, *Nanomedicine* **2008**, *3*, 183.
- [254] A. Liu, C. Li, H. Bai, G. Shi, *J. Phys. Chem. C* **2010**, *114*, 22783.
- [255] C. B. Parker, A. S. Raut, B. Brown, B. R. Stoner, J. T. Glass, *J. Mater. Res.* **2012**, *27*, 1046.
- [256] C. L. Kolarcik, K. Catt, E. Rost, I. N. Albrecht, D. Bourbeau, Z. Du, T. D. Y. Kozai, X. Luo, D. J. Weber, X. T. Cui, *J. Neural Eng.* **2015**, *12*, 16008.
- [257] G. Z. Chen, M. S. P. Shaffer, D. Coleby, G. Dixon, W. Zhou, D. J. Fray, A. H. Windle, *Adv. Mater.* **2000**, *12*, 522.
- [258] A. K. Geim, K. S. Novoselov, *Nat. Mater.* **2007**, *6*, 183.
- [259] Y. Wang, Z. Li, J. Wang, J. Li, Y. Lin, *Trends Biotechnol.* **2011**, *29*, 205.
- [260] X. Luo, C. L. Weaver, S. Tan, X. T. Cui, *J. Mater. Chem. B* **2013**, *1*, 1340.
- [261] C. L. Weaver, J. M. LaRosa, X. Luo, X. T. Cui, *ACS Nano* **2014**, *8*, 1834.
- [262] Y. Zhang, T. R. Nayak, H. Hong, W. Cai, *Nanoscale* **2012**, *4*, 3833.
- [263] Y. Liu, Y. Zhao, B. Sun, C. Chen, *Acc. Chem. Res.* **2013**, *46*, 702.
- [264] G. C. McConnell, H. D. Rees, A. I. Levey, C.-A. Gutekunst, R. E. Gross, R. V Bellamkonda, *J. Neural Eng.* **2009**, *6*, 56003.
- [265] T. Vermonden, R. Censi, W. E. Hennink, *Chem. Rev.* **2012**, *112*, 2853.
- [266] E. A. Appel, X. J. Loh, S. T. Jones, F. Biedermann, C. A. Dreiss, O. A. Scherman, *J. Am. Chem. Soc.* **2012**, *134*, 11767.
- [267] D. Seliktar, *Science* **2012**, *336*, 1124.
- [268] K. J. Lampe, R. G. Mooney, K. B. Bjugstad, M. J. Mahoney, *J. Biomed. Mater. Res. Part A* **2010**, *15*, 1162.
- [269] L. A. Flanagan, Y.-E. Ju, B. Marg, M. Osterfield, P. A. Janmey, *Neuroreport* **2002**, *13*, 2411.
- [270] V. Keskar, N. W. Marion, J. J. Mao, R. A. Gemeinhart, *Tissue Eng. Part A* **2009**, *15*, 1695.
- [271] R. M. Namba, A. A. Cole, K. B. Bjugstad, M. J. Mahoney, *Acta Biomater.* **2009**, *5*, 1884.
- [272] E. R. Aurand, K. J. Lampe, K. B. Bjugstad, *Neurosci. Res.* **2012**, *72*, 199.
- [273] Y. Lu, D. Wang, T. Li, X. Zhao, Y. Cao, H. Yang, Y. Y. Duan, *Biomaterials* **2009**, *30*, 4143.
- [274] L. Rao, H. Zhou, T. Li, C. Li, Y. Y. Duan, *Acta Biomater.* **2012**, *8*, 2233.
- [275] J. O. Winter, S. F. Cogan, J. F. Rizzo, *J. Biomed. Mater. Res. Part B Appl. Biomater.* **2007**, *81B*, 551.
- [276] D.-H. Kim, D. C. Martin, *Biomaterials* **2006**, *27*, 3031.
- [277] T. Nyberg, O. Inganäs, H. Jerregård, *Biomed. Microdevices* **2002**, *4*, 43.
- [278] M. Sasaki, B. C. Karikkineth, K. Nagamine, H. Kaji, K. Torimitsu, M. Nishizawa, *Adv. Healthcare Mater.* **2014**, 1919.
- [279] R. T. Hassarati, W. F. Dueck, C. Tasche, P. M. Carter, L. A. Poole-Warren, R. A. Green, *IEEE Trans. Neural Syst. Rehabil. Eng.* **2014**, *22*, 411.
- [280] D.-H. Kim, J. A. Wiler, D. J. Anderson, D. R. Kipke, D. C. Martin, *Acta Biomater.* **2010**, *6*, 57.
- [281] D.-H. Kim, M. Abidian, D. C. Martin, *J. Biomed. Mater. Res.* **2004**, *71A*, 577.
- [282] J. A. Chikar, J. L. Hendricks, S. M. Richardson-Burns, Y. Raphael, B. E. Pfingst, D. C. Martin, *Biomaterials* **2012**, *33*, 1982.
- [283] S. De Faveri, E. Maggiolini, E. Miele, F. De Angelis, F. Cesca, F. Benfenati, L. Fadiga, *Front. Neuroeng.* **2014**, *7*, 7.
- [284] Y. Lu, Y. Li, J. Pan, P. Wei, N. Liu, B. Wu, J. Cheng, C. Lu, L. Wang, *Biomaterials* **2012**, *33*, 378.
- [285] S. R. Shin, C. Shin, A. Memic, S. Shadmehr, M. Miscuglio, H. Y. Jung, S. M. Jung, H. Bae, A. Khademhosseini, X. S. Tang, M. R. Dokmeci, *Adv. Funct. Mater.* **2015**, *25*, 4486.
- [286] C. Hou, Y. Duan, Q. Zhang, H. Wang, Y. Li, *J. Mater. Chem.* **2012**, *22*, 14991.
- [287] H. Ding, M. Zhong, Y. J. Kim, P. Pholpabu, A. Balasubramanian, C. M. Hui, H. He, H. Yang, K. Matyjaszewski, C. J. Bettinger, *ACS Nano* **2014**, *8*, 4348.
- [288] J. Yi, Z. Zhao, S. Li, Y. Yin, X. Wang, *J. Wuhan Univ. Technol. Sci. Ed.* **2016**, *31*, 925.
- [289] L. He, D. Lin, Y. Wang, Y. Xiao, J. Che, *Colloids Surfaces B Biointerfaces* **2011**, *87*, 273.
- [290] T. Gabay, M. Ben-David, I. Kalifa, R. Sorkin, Z. R. Abrams, E. Ben-Jacob, Y. Hanein, *Nanotechnology* **2007**, *18*, 35201.
- [291] M. R. Abidian, J. M. Corey, D. R. Kipke, D. C. Martin, *Small* **2010**, *6*, 421.
- [292] Y. Lu, T. Li, X. Zhao, M. Li, Y. Cao, H. Yang, Y. Y. Duan, *Biomaterials* **2010**, *31*, 5169.
- [293] R. Gerwig, K. Fuchsberger, B. Schroepel, G. S. Link, G. Heusel, U. Kraushaar, W. Schuhmann, A. Stett, M. Stelzle, *Front. Neuroeng.* **2012**, *5*, 8.
- [294] A. Liu, C. Li, H. Bai, G. Shi, *J. Phys. Chem. C* **2010**, *114*, 22783.
- [295] X. Luo, C. L. Weaver, S. Tan, X. T. Cui, *J. Mater. Chem. B* **2013**, *1*, 1340.
- [296] D. H. Kim, J. A. Wiler, D. J. Anderson, D. R. Kipke, D. C. Martin, *Acta Biomater.* **2010**, *6*, 57.
- [297] S. F. Cogan, *Annu. Rev. Biomed. Eng.* **2008**, *10*, 275.
- [298] D. A. Borton, M. Yin, J. Aceros, A. Nurmikko, *J. Neural Eng.* **2013**, *10*, 26010.